NASA Contractor Report 3983

Investigation of Interactions Between Limb-Manipulator Dynamics and Effective Vehicle Roll Control Characteristics

D. E. Johnston and D. T. McRuer
Systems Technology, Inc.
Hawthorne, California

Prepared for
Ames Research Center
Dryden Flight Research Facility
under Contract NAS2-11454

National Aeronautics
and Space Administration

**Scientific and Technical
Information Branch**

1986

TABLE OF CONTENTS

LIST OF FIGURES

LIST OF FIGURES (Continued)

LIST OF FIGURES (Concluded)

LIST OF TABLES

LIST OF SYMBOLS

A	Analog
a_y	Lateral Acceleration
D	Digital
DFRF	Dryden Flight Research Facility
dB	Decibel, 20 $\log_{10}()$ for Amplitude Ratio; 10 $\log_{10}()$ for Power
F_A	Roll Stick Force
F_{as}	Roll Control Stick Force, Positive Right
GM	Gain Margin
Hz	Frequency Measure in Cycles Per Second
K	System Gain
K_c	Controlled Element Gain; Command/Force Gradient
K_p	Pilot Gain
L'_{FAS}	Effective Roll Acceleration Coefficient Per Unit Roll Manipulator Force Input
ms	Millisecond
n	Number of Runs
NM/L	Neuromuscular and Limb System
P	Roll Rate
P_c	Roll Rate Command
PIO	Pilot Induced Oscillations
P_{ss}	Steady State Roll Rate
RMS (rms)	Root Mean Square
s	Laplace Transform Variable
T	Controlled Element First-Order Time Constant

LIST OF SYMBOLS (Concluded)

T_F	Command Prefilter Lag Time Constant
T_N	Neuromuscular Mode First-Order Time Constant
T_r or T_R	Roll Time Constant
Y_c	Controlled Element Transfer Function
Y_p	Pilot Describing Transfer Function
δ	Stick or Control Surface Command
ΔAR	Neuromuscular Peak Amplitude Ratio Departure from Y_pY_c Bode Asymptote
ζ	Damping Ratio Terms
σ	Standard Deviation
σ_e	Task RMS Error
τ	Time Delay
ϕ	Roll Response Angle
ϕ_e	Rolling Response Error
ϕ_M	Phase Margin
ω	Angular Frequency
ω_c	Closed-Loop Bandwidth (Crossover of the 0 dB Gain Line with the K/s Amplitude Ratio Plot)
$\omega_c\sigma_e$	Product of Crossover Frequency and RMS Error (Perforamcne Measure)
ω_i	Nominal Bandwidth of the Forcing Function Spectrum
ω_N	Neuromuscular Second-Order Mode Frequency
ω_u	Frequency at Which System Becomes Unstable (ϕ = 180°)
$\measuredangle$	Angle

SECTION I

INTRODUCTION

From the earliest studies on the interaction between the human pilot's neuromuscular system and aircraft control devices (e.g., Refs. 1 and 2) the presence of a neuromuscular system limb-manipulator dynamic resonance peak at 14-19 rad/sec has been well known. In Ref. 3 the neuromuscular system characteristics are cited as "exceptionally important and critically limiting in such matters as

- control precision where limited by the pilot's neuromuscular system dynamics.
- effects of control system nonlinearities, including their connections with control system sensitivity requirements."

Reference 4 and other summaries place great stress on the importance of considering these characteristics even though this frequency range of major activity may be well above the bandwidth associated with the "usual" control task.

It is becomming more and more apparent that modern, high performance, high gain, command response flight control system bandwidths may be encroaching on the neuromuscular system. Advances in flight control system fly-by-wire technology permit new manipulation devices, for example force sensing side-sticks, at the pilot output/effective-vehicle interface. These have thus far been generally successful in application, but have introduced or enlarged some pilot-vehicle flying qualities problems. Particular problems include:

- high roll control sensitivity and PIO's in precision maneuvering;
- roll ratchet in otherwise steady rolling maneuvers;
- sensitivity to the way the pilot grips the stick or to location of his hand/arm support;
- effective time delay associated with stick filters, with attendant increase in pilot remnant;

- biodynamic interactions, e.g., hand/arm stick bobweight effects.

Attempts to alleviate these effects have involved adjustments in stick force gradients, filtering, and sensitivity. These have included introduction of various nonlinear elements such as command gain reduction as a function of pilot input amplitude or frequency, filter time constant changes with sense of input (increase vs. decrease), and different force gradient for right and left roll commands. These adjustments have generally involved ad hoc empirical modifications in the course of the aircraft development. Much of this has been accomplished in flight test with correspondingly large cost.

Thus there is a need to revisit and expand the earlier neuromuscular system experimentation with a focus on now-practical flight control system configurations in order to quantify possible interactions between these and the neuromuscular system. The result should provide a first cut at manipulator/flight control system design guides and criteria to minimize roll control problems. The experimental program documented herein was undertaken to satisfy these goals.

In the section which follows the background is reviewed covering various roll control problems, results of specific flight test investigations, and previous observations concerning the neuromuscular system dynamic characteristics. This sets the stage for definition of experiment goals and setup for this program which are presented in Section III.

The experiment encompassed some 96 manipulator/controlled-element configurations involving over 530 runs by two subjects. Key findings are summarized in Section IV. These show a strong correlation with previous flight test results, identify the neuromuscular system as potentially involved in roll ratchet, indicate manipulator, response command, and effective vehicle dynamics which aggravate the nuisance neuromuscular dynamics, and provide a measurement procedure for assessing the potential of roll ratchet using fixed-base simulation.

Conclusions and recommendations for further experimentation are contained in Section V.

SECTION II

BACKGROUND FOR STUDY

Almost every new aircraft with fly-by-wire or command augmentation in the roll axis has encountered either Pilot-Induced Oscillations (PIO) or roll ratcheting (or both) in early flight phases. PIO has typically been associated with high gain, neutrally stable closed-loop pilot-vehicle control oscillations with a frequency of about 1/2 Hz. The "roll ratchet" has been somewhat more obscure and idiosyncratic, appearing most often in rapid rolling maneuvers. Ratchet frequencies are typically 2-3 Hz. Figure 1 illustrates this oft-remarked but seldom recorded phenomenon. The frequency difference alone indicates that the PIO and ratchet situations are different phenomena, yet both clearly involve the closed-loop pilot vehicle system.

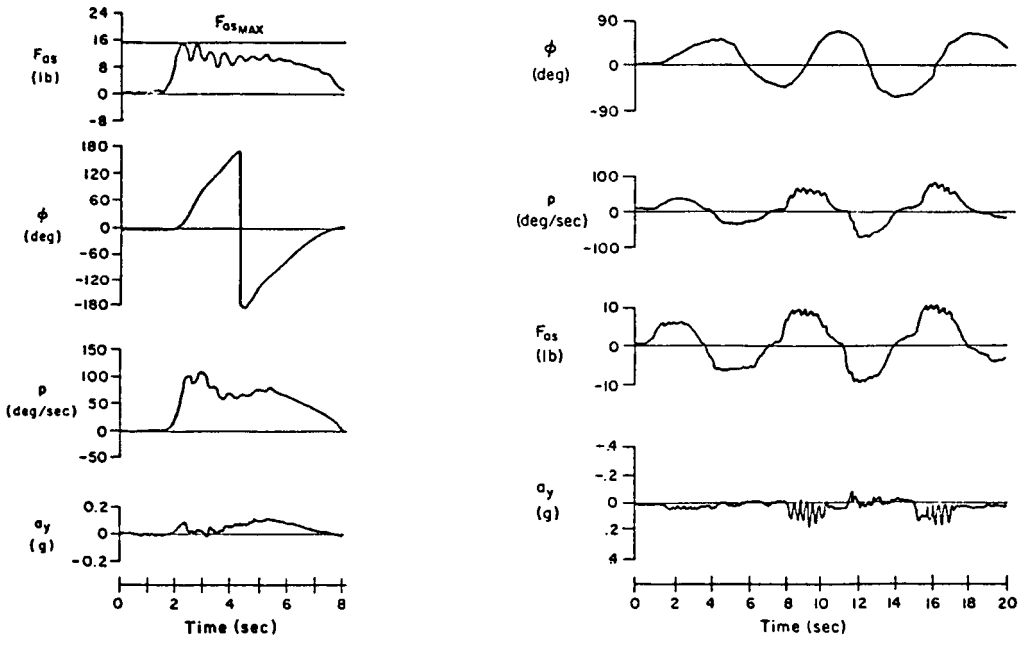

a) F-16 *b) Aircraft A, CAS I*

Figure 1. Roll Ratchet During Banking Maneuver

SOME FLYING QUALITIES OBSERVATIONS

An interesting set of roll ratcheting phenomena occurred in the flight tests of Refs. 5-7. The oscillations were 11-17 rad/sec in these cases. Chalk (Ref. 8) speculates that the oscillations were due to the near K_c/s character of the effective controlled element. He used a rudimentary ($K_p e^{-\tau s}$) non-adaptive pilot model to show that one can get an instability at about 12-17 rad/sec with a K/s-like aircraft and high pilot gains. The phase margin for the open-loop pilot-aircraft system in this case is

$$\phi_M = \frac{\pi}{2} - \tau\omega_c$$

The instability corresponds to $\phi_M = 0$, so the value of τ corresponding to the neutrally stable frequency, $\omega_c = \omega_u$, will be

$$\tau = \frac{\pi}{2\omega_u}$$

Accordingly, the effective τ corresponding to oscillations of 12 to 17 rad/sec will be in the range from 0.09 to 0.13 sec. This effective time delay must account for <u>all</u> the open-loop system lags, i.e., controller, actuator, filters, etc., plus the effective latency of the pilot. So, if this explanation of the roll ratchet is to be reasonable the total τ value must be appropriate. The 0.09 - 0.13 second range is remarkably low for the pilot alone, and is very low indeed when aircraft plus control system effective lags are also considered.

In Ref. 9, Mitchell and Hoh also examine some of the same data. They cite the sinusoidal vibration data of Ref. 10 in which a simple lateral tracking task was performed (using a center stick) while under the influence of high frequency lateral accelerations. Frequencies from 1 to 10 Hz were employed and an oscillatory arm/stick "bobweight" mode occurred at about 12 rad/sec. They note that this higher frequency mode of the pilot-aircraft systems is near the frequencies of the observed ratcheting in the F-16 and Calspan flight experiments and cite it as a possible cause.

SOME PILOT-VEHICLE SYSTEM CONSIDERATIONS

The prescription for K/s-like controlled element dynamics in the region of pilot-vehicle system crossover as an often desirable form stems from the fundamental feature of human dynamics that no pilot lead is then required to establish good closed-loop dynamics over a wide range of pilot gains. The basic recipe is almost invariably conditioned by such statements as "in the frequency region about crossover." Such statements are made to restrict the form of the pilot model to that required only in the crossover region. In particular, the cases covered are such that an effective time delay term in the pilot model is an adequate approximation to the high frequency effects.

Simple tracking task pilot model forms and associated pilot-vehicle system properties begin with the ideal crossover model of Fig. 2 (see e.g., Ref. 4). In this model the pilot adjusts his dynamic characteristics so that the open-loop pilot-vehicle dynamics are approximately K/s over the frequency band immediately above and below the gain crossover. The model also indicates that in full attention tracking operations the pilot will adjust his gain to offset any variation in controlled element gain in order to maintain a nearly fixed control system bandwidth. Thus the full-attention closed-loop bandwidth ω_c (identified as the crossover of the 0 dB gain line with the K/s amplitude ratio plot) is independent of the controlled element gain. Furthermore, the pilot tends to keep the product of the crossover frequency and the task RMS error, $\omega_c \sigma_e$, constant.

In the crossover model the exponential term with time delay τ approximates all the lag contributions due to pilot and vehicle high frequency dynamic modes. The effective time delay is a function of, among other things, the force/displacement characteristics of the manipulator. As shown in Fig. 2, an isometric (force) stick results in less lag than does an isotonic (free moving) stick. Past experimentation has identified the difference to be approximately 0.1 sec (e.g., Ref. 4).

In Fig. 2 if the pilot gain were set at the value represented by K_{p2} with an isometric stick, the bandwidth would be indicated by ω_{c2} and

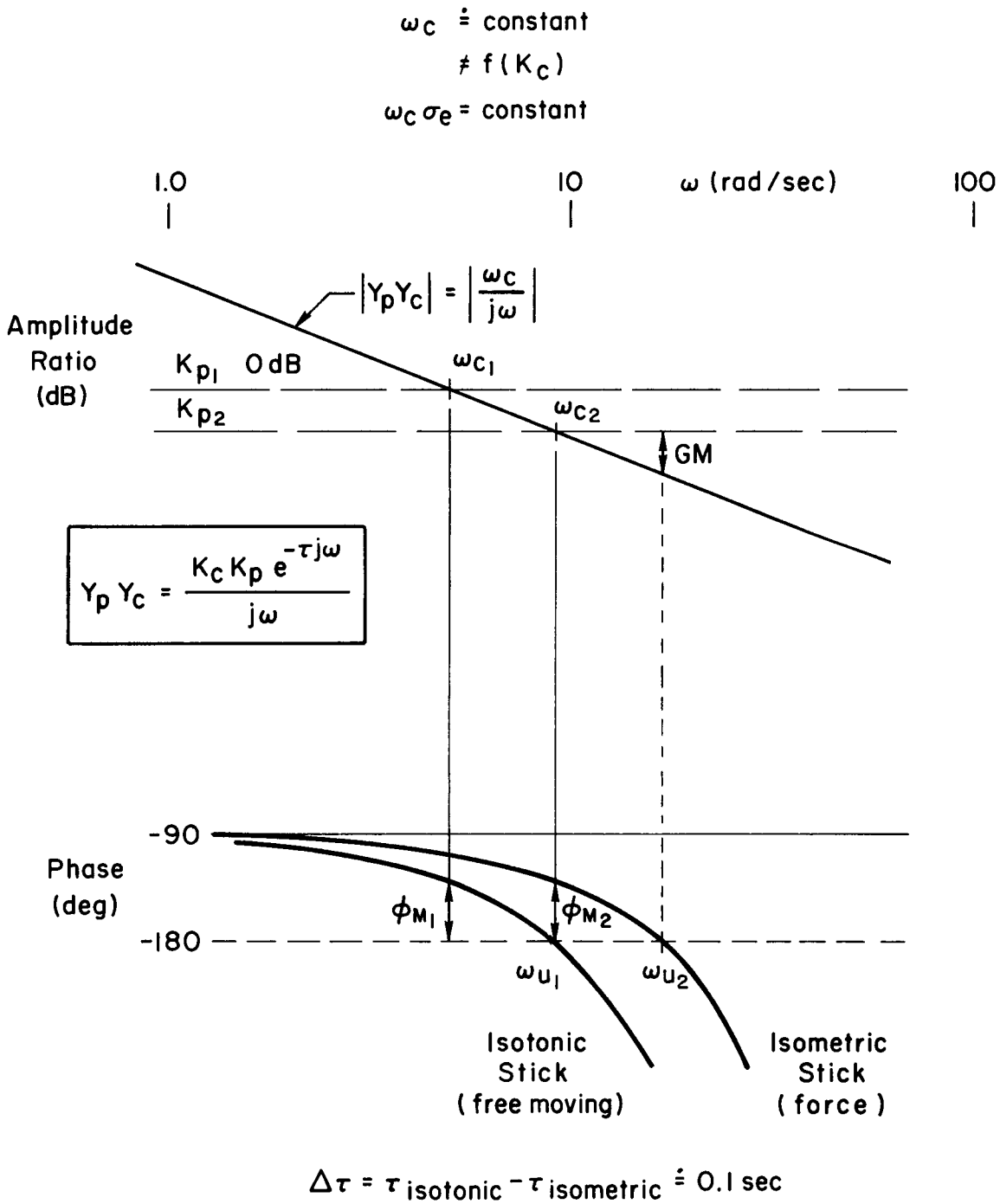

Figure 2. Ideal Crossover Model

would result in a system stability phase margin, ϕ_{m2}, and gain margin, GM. If this same gain were employed with the isotonic stick, the phase margin would be 0, and a low frequency continuous oscillation (PIO) would result. This oscillation can then be alleviated by the pilot reducing his gain to the value represented by K_{p1} and accepting the reduced bandwidth. Thus Fig. 2 can be used to demonstrate the common low frequency PIO problem which generally occurs in the vicinity of 0.5 Hz and which is relieved by reducing pilot gain. (In the crossover model an ω_u of 4 rad/sec corresponds to $\tau = \pi/2\omega_u \doteq 0.4$ sec for the total pilot, control system, aircraft, etc., latency).

As previously noted, early studies on the neuromuscular system (e.g., Ref. 1 circa 1968) noted the presence of a neuromuscular system or limb-manipulator peak at 14-19 rad/sec well past the usual "crossover region." The effects of various restraints on the limb/neuromuscular system are described in detail in Ref. 2. Figure 3 (from Ref. 2) shows closed-loop neuromuscular system model fits to pilot/controlled-element describing function measurements for pressure and free moving manipulators. An important part of the neuromuscular dynamics in each case is a quadratic mode with damping and natural frequency of

MANIPULATOR	NM/L DYNAMICS
Free Moving	[0.07, 17]
Isometric or Pressure	[0.138, 18.6]

The experiments which allowed identification of these modes used forcing functions having a low power shelf extending to higher frequencies than normally utilized in tracking tasks. The human pilot describing function data of Fig. 4 from Ref. 11, provides an example of the range of frequencies needed to completely define the resonant peak. Note in Fig. 3 that there is a second neuromuscular system mode which is approximated by a first-order lag break at about 10 rad/sec. This mode is also somewhat dependent on the nature of the manipulator restraints (Refs. 12 and 13).

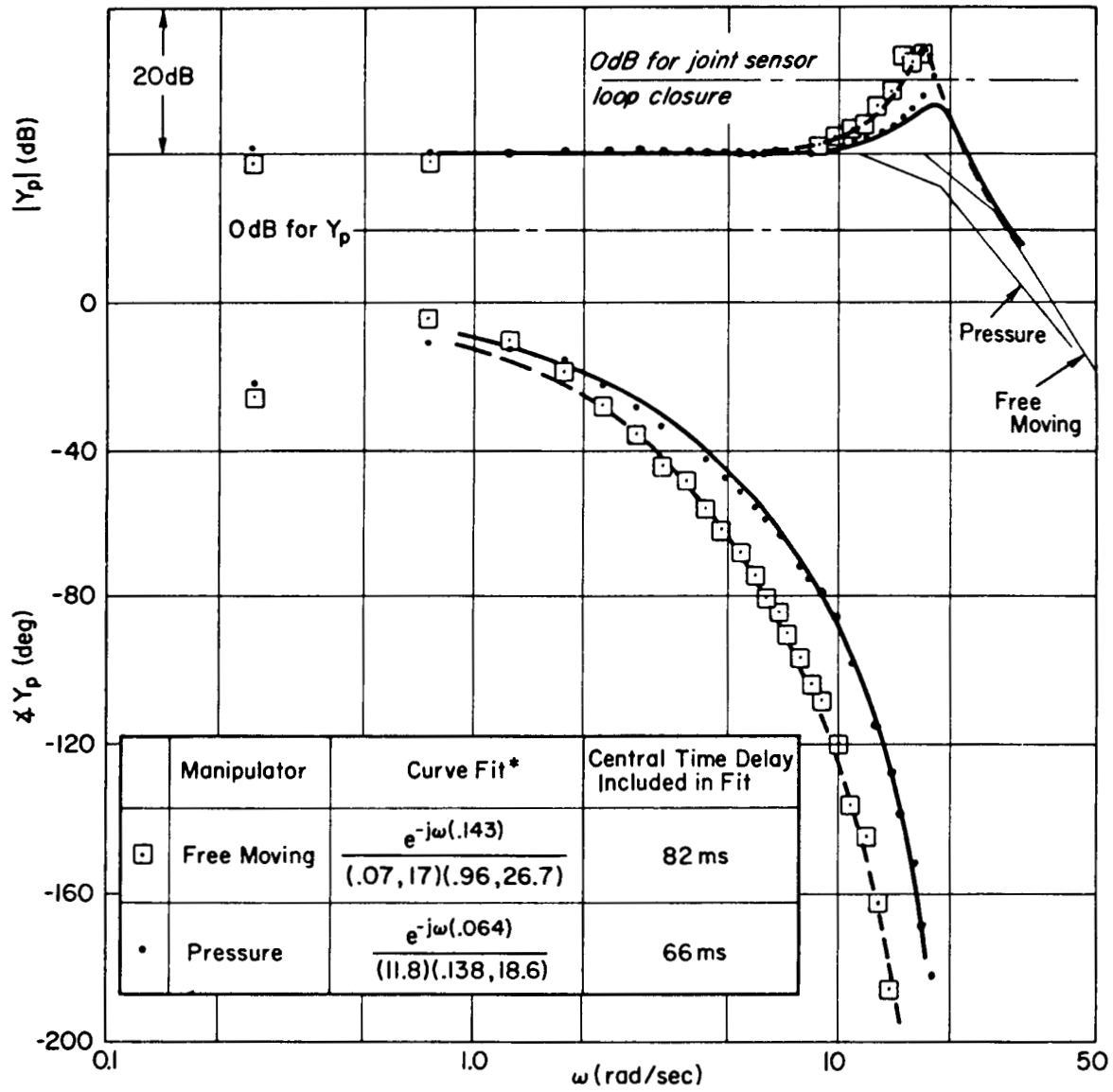

*Note: To simplify the notation, $(s^2 + 2\zeta\omega s + \omega^2)$ is written (ζ, ω) and $(s + a)$ is written (a).

Figure 3. Closed-Loop Neuromuscular System Model Fit to Y_p for Pressure and Free-Moving Manipulator ($Y_c = 1/s$) from Ref. 2

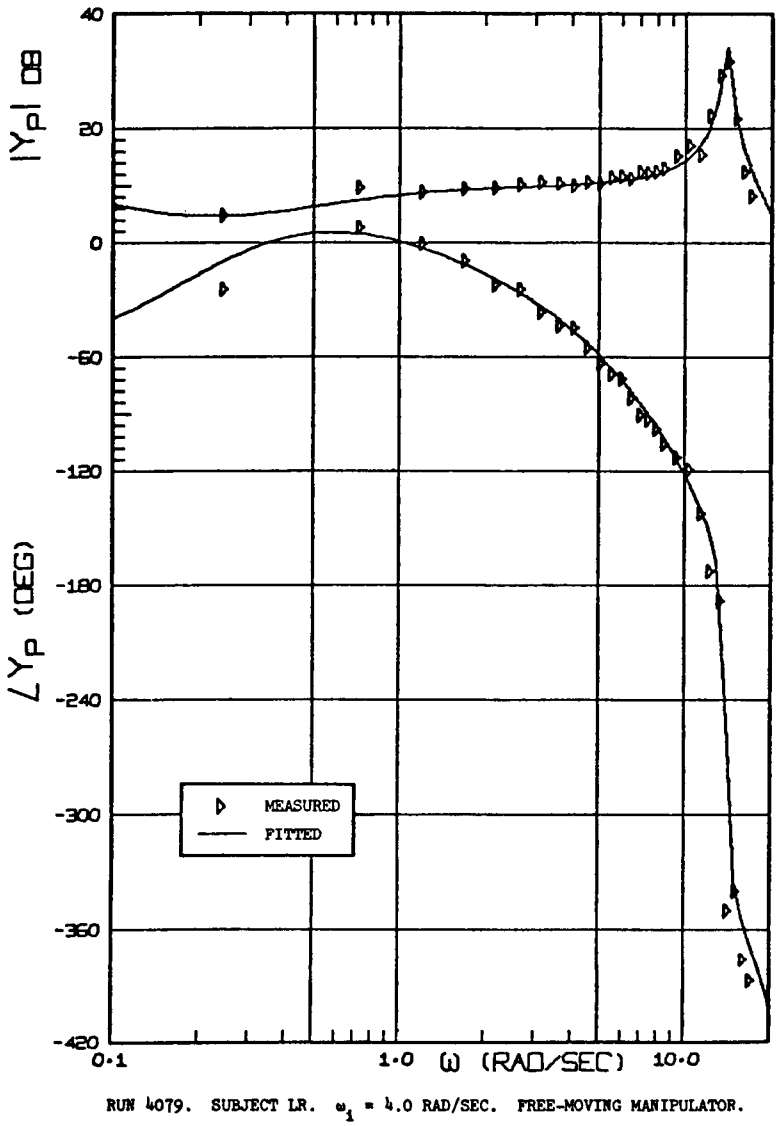

Figure 4. Example Describing Function Showing High Frequency Peak (Taken from Gordon-Smith, Ref. 11)

The reason that the neuromuscular actuation system dynamics differ when the manipulator restraints are changed is physiological -- the neuromuscular apparatus involved depends on the restraints and limb movements. While greatly oversimplified, the neuromuscular actuation elements of the human may be viewed as a two loop system. The inner loop principally involves Golgi and muscle spindle receptors with short pathways directly to spinal level and back to the musculature. Viewed from the output end this loop is primarily sensitive to forces, and because of the short neural pathways the time lags of information flow are small. The effective bandwidth of this loop can, therefore, be quite high. The second or outer loop includes joint and other (e.g., peripheral vision) receptors as major feedback elements. Their neural pathways, and associated delays, are longer, leading to a lower outer loop bandwidth. In isometric (force-stick) manipulator conditions, there is little or no joint movement, so the inner loop elements should be dominant. With isotonic (free-moving stick) conditions, on the other hand, the joint receptors are major elements. As already indicated in connection with Fig. 2 the net difference, in terms of an effective latency, is approximated at low frequencies by a difference in effective τ of about 0.1 sec.

If we now employ the Fig. 3 detailed model of the neuromuscular system (instead of only approximating its phase lag contribution as in Fig. 2) and superimpose it on the controlled element K/s as in Fig. 5, we see an open-loop resonant peak in the 2 to 3 Hz frequency range due to the neuromuscular system. The correspondence of the neuromuscular/limb quadratic mode numerical values and observed roll ratchet frequencies is very unlikely to be a coincidence. So, at observed roll ratchet frequencies the neuromuscular/limb mode clearly should be taken into account. Since their primary effect is a resonant peak from which "Gain Margin" might be measured,* it is quite apparent that these properties will be of central importance for high gain pilot situations.

*While the "Gain Margin" shown in Fig. 5 indicates the magnitude difference between the $|Y_pY_c|_{dB}$ peak and the zero dB line, the phase at or near this frequency may differ appreciably from that required for instability. Thus when the "Gain Margin" shown is zero only one of the two conditions for instability may be satisfied. Consequently this is not necessarily a true gain margin in the conventional sense. It does, however, indicate a resonant tendency contributed by the pilot.

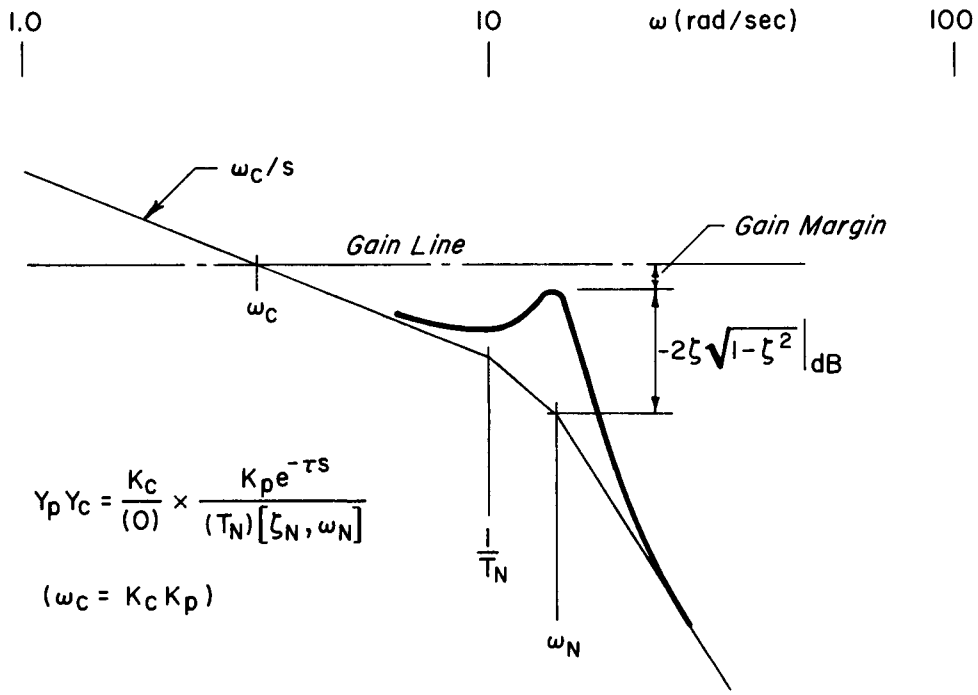

Figure 5. Bode Amplitude Ratio Plot for Neuromuscular System Contribution to Roll Ratchet Potential

F-16 DATA ON ROLL RATCHET

Although no frequencies are cited, information provided in the Ref. 14 summary of the F-16 side stick controller/roll prefilter development lends support to the neuromuscular system mode as a key factor in roll ratchet. This report summarizes a 155 flight, 34 pilot program evaluating 19 different side stick and prefilter configurations in the YF and F-16A aircraft accomplished over a period of 5 years. Of these 155 flights, 74 were devoted to stick displacement, force gradient, and input axis orientation considerations while 81 were devoted to roll prefilter configurations.

The initial prefilter was a non-linear filter which provided a 0.4 sec time constant (or $1/T_F = 2.5$) for command inputs and a 0.1 sec time constant (or $1/T_F = 10$) for removal of the commands. This was denoted as the 0.4/0.1 prefilter. During flights with this prefilter, roll ratcheting was noted in moderate rate 360 deg rolls, decreasing

roll rate rolls, formation flying, etc. The roll ratcheting was characterized as high frequency lateral oscillations which were attributed partially to physiological feedbacks of aircraft motion through the inertia of the pilot's hand and his grasp of the controller. However, these were not all necessarily high acceleration maneuvers where hand inertia might lead to inadvertent force inputs.

During the course of the F-16 program the pilots stated that the grip on the side stick controller was too large in diameter to allow a comfortable grasp. Rolls to the right were uncomfortable because only the right thumb was available to supply the right roll force while the entire palm of the hand was available for rolls to the left. Interestingly, the F-16 roll ratchet time traces shown in both Refs. 8 and 9 are for a roll to the right (see Fig. 1a) and a second set of roll reversal maneuver time traces in Ref. 9 for another aircraft shows a much larger amplitude roll ratchet for right rolls versus left rolls (see Fig. 1b). The F-16 ratchet was at 12-13 rad/sec while the second aircraft was at 18 rad/sec. In both cases the stick prefilter time constant was 0.1 sec and stick forces are about 10-12 lb. The response to command ratio appears to be in the vicinity of 6 to 7.5 deg/sec/lb.

It is shown in Ref. 15 that the frequency of the neuromuscular mode increases and damping decreases as muscular tension increases. Figure 6 is adopted from that reference. Note the locus near the origin is a second-order mode [ζ_N, ω_N] that can be driven to zero damping or even a divergence with increasing "gain" (large muscle tension). This could be a contributory factor in the above noted F-16 ratchet during rolls to the right since it requires considerably greater tension of the thumb to command right roll than of the hand to command left roll even though the same force is generated in both directions. Also note in Fig. 6 the previously mentioned first-order lag, $1/T_{N_1}$, of the neuromuscular system which moves toward the zero at about 10 rad/sec. Therefore its lag contribution also shows up at lower and lower frequency as muscle tension is increased.

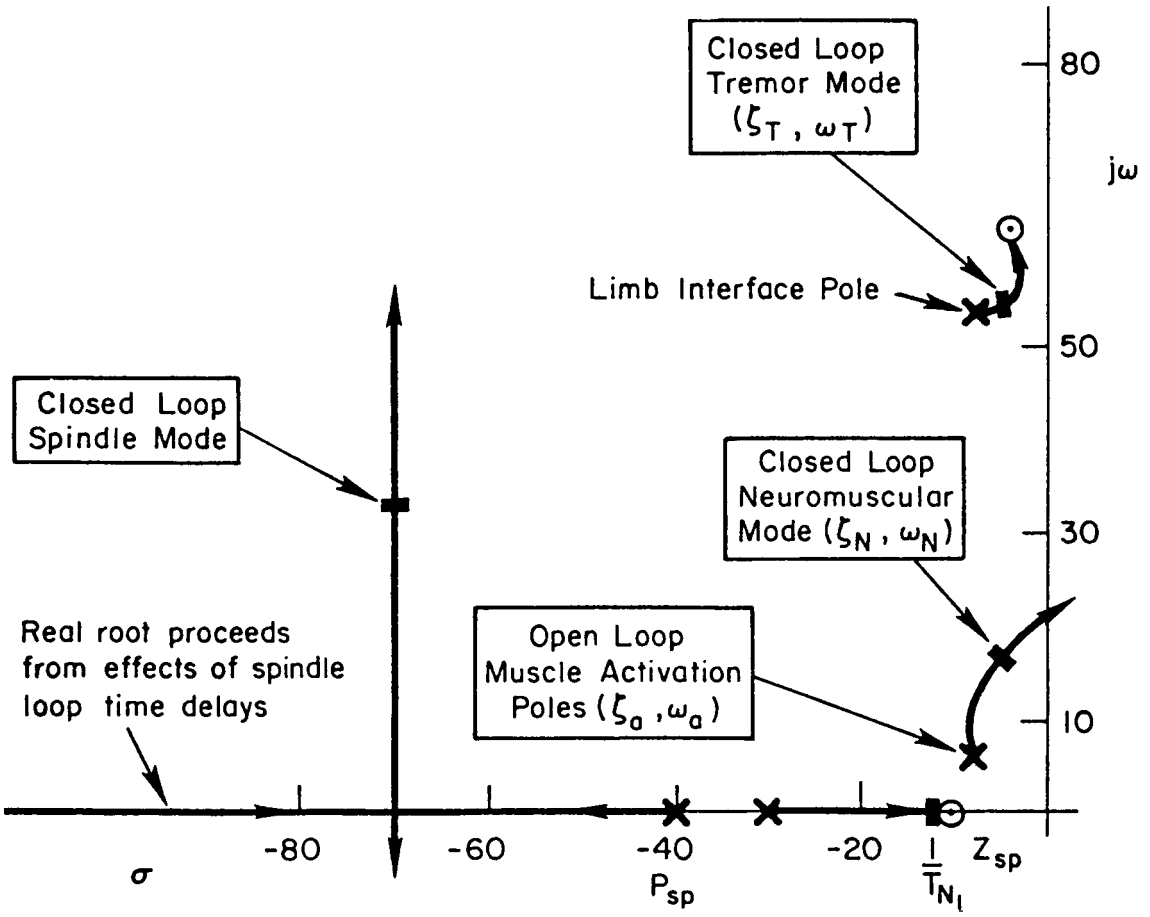

Figure 6. Root Locus Diagram Showing Modes for "Spindle" (Inner) Loop Closure of Neuromuscular Loop as Average Neuromuscular Tension is Increased (Adopted From Ref. 15)

It is reported in Ref. 9 that a second roll maneuver similar to that shown in Fig. 1a was flown a few seconds after the maneuver shown here and the roll ratcheting was not present. Thus the idiosyncratic nature of the phenomenon. Other flight test programs, for example Ref. 6 flown with a force sensing center-stick, found that the roll ratcheting was sensitive to pilot aggressiveness and could be alleviated by "backing off" (lowering gain).

In summary, the observed roll ratcheting occurs at frequencies commensurate with the neuromuscular system natural frequency and may be aggravated by the muscular tension required to generate force primarily

with the thumb (right rolls) rather than the palm of the hand (left rolls). It could also be associated with limb-manipulator mechanical bobweight coupling at high roll accelerations.

SIDESTICK FORCE/DISPLACEMENT FLIGHT DATA

An experimental program to investigate the influence of side-stick force, displacement, and command gradient characteristics on aircraft flying qualities is reported in Ref. 16. This was flown in the Calspan NT-33 aircraft using a roll rate command system. The roll rate command vs. stick force gradients investigated in this flight program are shown by the dashed lines in Fig. 7. Four different command/force gradient configurations were flown. These were rated as light (L), medium (M), heavy (H), and very heavy (VH). In each case the breakout force is approximately 1 lb. This is followed by an initial slope having high force to roll rate command gradient. At 3 lb force a second gradient begins which has lower force to roll rate command ratio. Also shown (solid lines) in Fig. 7 are two sets of gradients employed in the F-16 flight investigation reported in Ref. 14. These also had about 1 lb breakout but were followed by a 3 segment gradient. The set identified as F-16 FDS were the original production gradients. The second set (identified as M3) are the best that could be obtained through simple modification of the F-16 flight control computer. Note these both have initial gradients which require much higher forces than used in the NT-33 up to roll rate commands of 20 deg/sec. Between 20 deg/sec and 80 deg/sec the force gradients for the F-16 are about the same as those identified as very heavy in the NT-33, but have an absolute force level some 3 lbs higher than in the NT-33. Above 80 deg/sec the production F-16 force/command gradient was less than that identified as light in the NT-33.

In addition to the different force/command gradients reflected in Fig. 7, the Ref. 16 flight test also investigated 3 different stick displacement configurations. One was a fixed (no displacement) stick as in the F-16, the second had 0.77 deg/lb (small) stick motion, and the third had 1.43 deg/lb (large) stick motion. Flying tasks included air-to-air

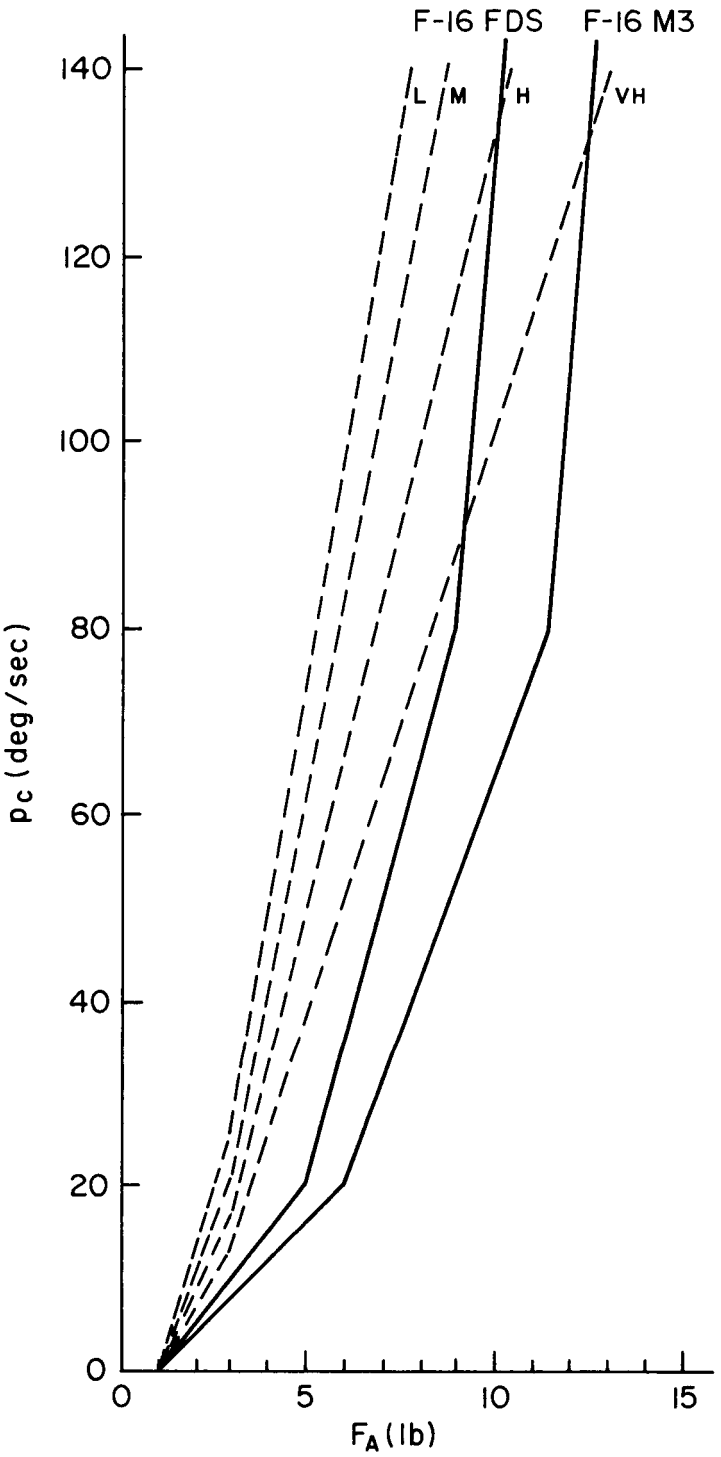

Figure 7. NT-33 and F-16 P Command Gradients
Up and Away Flight

tracking, formation, gross maneuvering, and landing. Figure 8 is a summary of the configurations evaluated in the air-to-air tracking task along with handling quality ratings given to each configuration and pertinent pilot comments. The scale on the left in Fig. 8 is roll rate command/force gradient (deg/sec/lb). At the bottom of Fig. 8 the different stick displacement characteristics are identified as F, S, and L. The placement of the circles identify the initial command/force gradients (below 3 lb) investigated with each of the stick configurations. The very heavy fixed-stick had an initial command/force gradient of 6.5 deg/sec/lb and the light configuration a gradient of 12.5 deg/sec/lb. For comparison, the x's for the fixed-stick identify the production F-16 force gradient at 4 deg/sec/lb and the modified gradient at 5 deg/sec/lb.

Numbers inside the circles are the handling quality ratings given to each of the configurations flown in the NT-33. Some caution must be exercised in employing these ratings because the pilot was evaluating both longitudinal and lateral stick characteristics. For example, the light gradient fixed-stick was given a handling quality rating of 8 apparently due to pitch control problems because there was no adverse comment about roll control.

The pilot comments reflected in Fig. 8 tend to indicate a preference for the medium force gradients for all 3 types of sticks although it is possible the light gradients with the fixed and small displacement stick may have been considered good also. The comments indicate the heavy and very heavy force gradients are undesirable because of the high forces required and reflect specific problems for roll to the right. While there are several references to jerky roll control the only actual reference to ratchet tendency occurs with the large deflection, low force gradient stick. This would be the configuration which comes closest to being a free moving or isotonic stick.

Figure 9 presents a similar summary for the various command/force gradient and stick motion configurations for the gross maneuvering task. For this case the second command/force gradient was selected because it is assumed that in gross maneuvering a higher roll rate would be commanded and therefore the lighter gradients would be involved. Again the

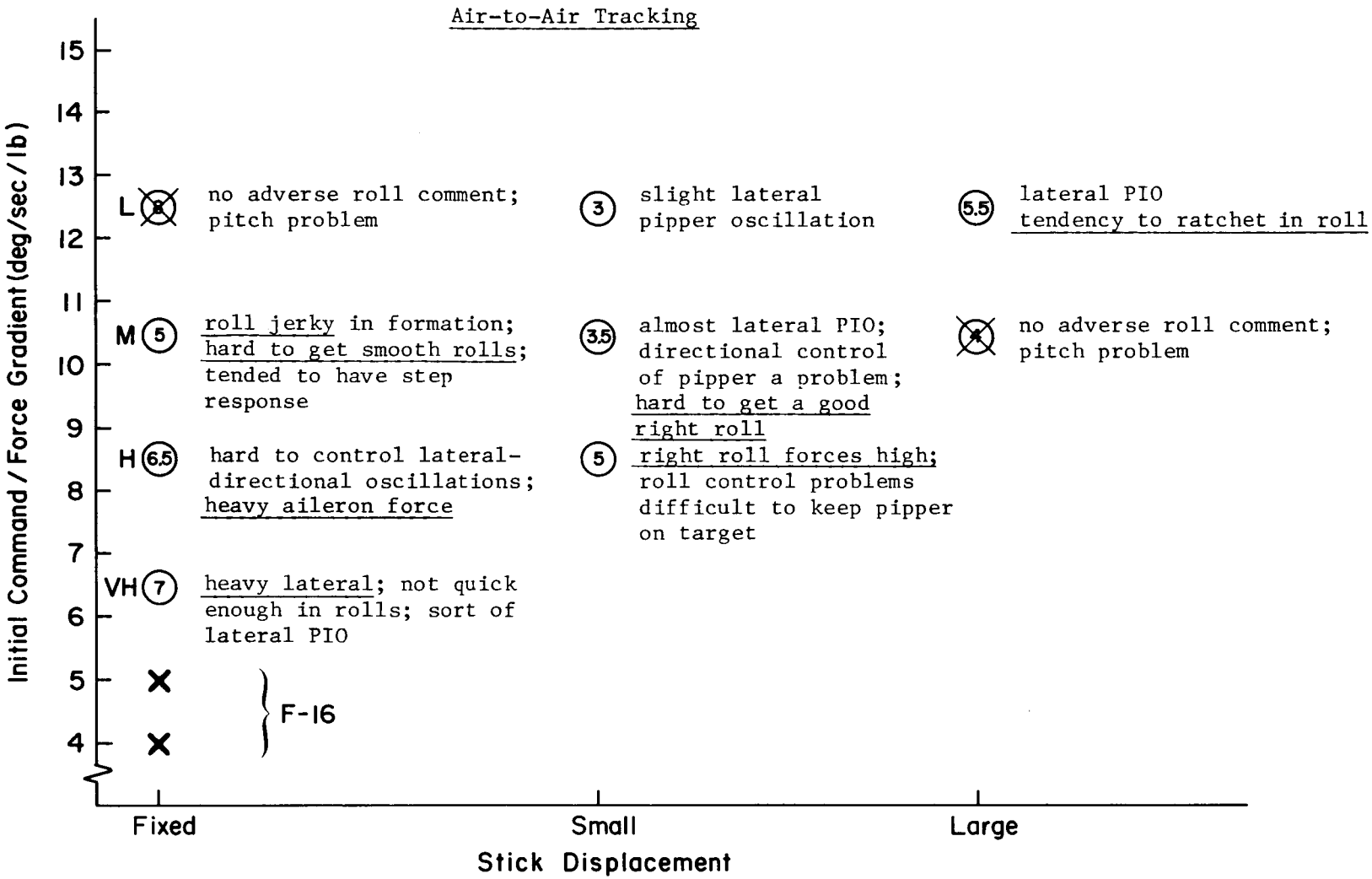

Figure 8. NT-33 Sidestick Configurations and Lateral Directional Control Comments for Air-to-Air Tracking

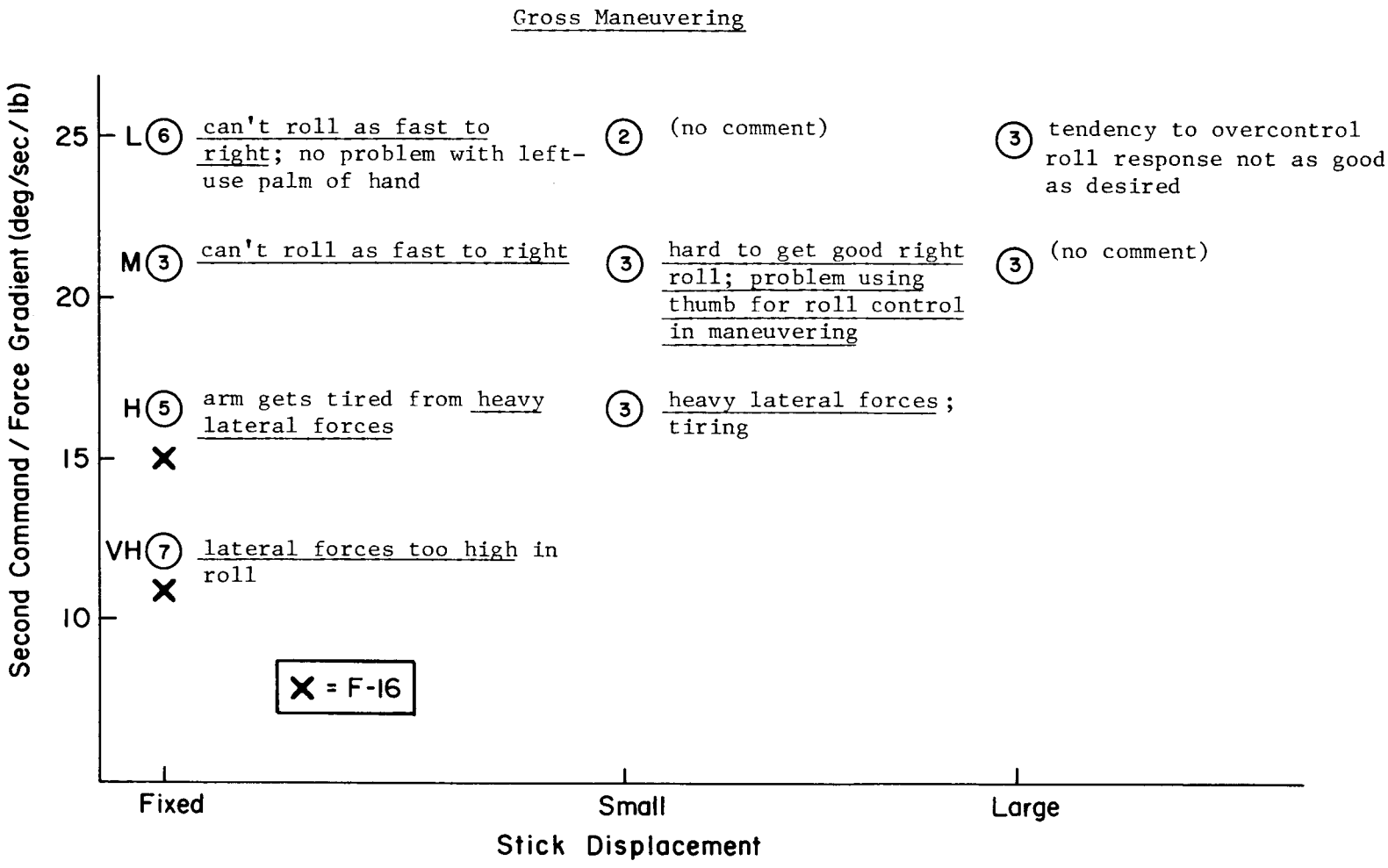

Figure 9. NT-33 Sidestick **Configurations** and Lateral Directional Control Comments for Gross Maneuvering

two F-16 configurations are identified with the x symbols, and are found to be close to the NT-33 very heavy and heavy configurations. The comments reflect general problems of excessive maneuvering forces and, in particular, problems in right rolls. However, there are no comments reflecting tendency to roll ratchet. For the fixed-stick configuration the handling quality ratings indicate only command/force gradient in the 20 to 21 deg/sec/lb region to be acceptable. On the other hand, the small stick deflection configuration reflects relative insensitivity to the command/force gradients flown. The same also appears true for the large deflection stick configuration. The consensus reflected in Ref. 16 is that the medium force gradients were considered a best compromise for all flying tasks.

The possibility of using different force/command gradients for right vs. left maneuvering was actually investigated in the F-16 (Ref. 14) where command gains for right rolls were greater than those for left rolls. Unfortunately the particular gradients selected were not acceptable to the pilots who could detect the different response/force characteristic and felt it actually degraded flying qualities and performance. No attempt was made to optimize the difference in gradients, so it is not really known whether such an approach could prove feasible.

In summary, the problems observed in various flight programs include sensitivity to command/force gradient and achieving the best compromise gradients for various mission phases and tasks. Specific complaints often center on jerky or step-like roll rate response when command gain is high and on generating sufficient thumb force to obtain adequate roll rates to the right when command gain is low. Jerkyness or ratchet tendency has generally been solved by increasing the prefilter lag (e.g., Ref. 14). This leads to the "normal" low frequency PIO. Solutions for this low frequency problem are to lower the command gain and to back off on the command filtering. Thus a compromise prefilter time constant is found for each individual manipulator. But, previous experimentation has shown that the manipulator itself might be altered to reduce neuromuscular ratchet tendency.

The search for answers to these problems led to our experimental plan.

SECTION III

EXPERIMENT GOALS AND SETUP

No accounts have been found where roll ratchet has been observed or recognized in fixed- or moving-base simulations. It apparently has only occurred in actual flight and then on a more or less random basis. The first objective of this experimental setup therefore was to tune the controlled element, manipulator, and command/force gradients to try to achieve roll ratchet, or at least maximize roll ratchet tendencies, in the fixed-base simulation. The experimental goals were to investigate and quantify limb/manipulator dynamics and interactions between the neuromuscular subsystem, force sensing side-stick configuration, high gain command augmentation, and command filtering; and to investigate possible relationships between these interactions and the roll ratchet phenomenon. Results should also provide a basis for future flight experiments with the DFRF digital F-8 aircraft. A longer range goal is to provide and enhance guidelines for manipulator-system design.

The experimental setup is depicted in Fig. 10. A roll tracking task was selected in which the pilot matches the bank angle of his controlled element with that of a "target" having pseudo random rolling motions. The random motions are obtained via a computer generated sum of sine waves. The error is displayed on a CRT and the pilot attempts to null the error by applying force to the manipulator, the output of which becomes the command to the controlled element, Y_c. The form of the controlled element is identified in Fig. 10 along with the range of lag time constants and time delays utilized in the experiment. This controlled element approximates a high gain roll rate command system. The time lag parameter, T, may be considered to be the effective roll subsidence time constant or a flight control system prefilter (between the pilot's stick command and the flight control system), whichever is larger. For very small values of τ the pure time delay may be a realistic approximation to digital flight control system sample and hold dynamics. More generally it is a low frequency approximation for all

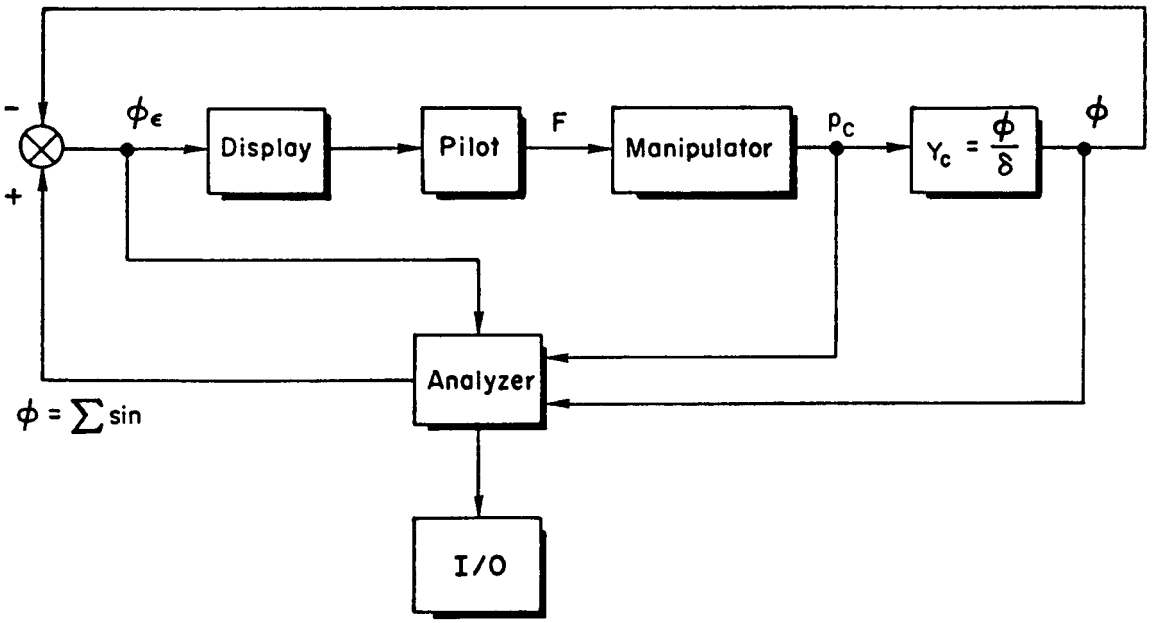

$$Y_C = \frac{K_C e^{-\tau s}}{s(Ts+1)} \quad ; \quad \begin{matrix} \tau = 0 \rightarrow 0.1 \\ T = 0 \rightarrow 0.4 \end{matrix}$$

Figure 10. Experimental Setup

the high frequency lags in the system which are not covered by the time lag T. Because we are interested primarily in modern flight control systems, the parameter values for T and τ used in the experiment are generally consistent with values that would be present in a system designed to be Level 1 on the basis of flying qualities specifications. Thus, the parameter values used, in the main, should produce excellent effective controlled elements providing the gain is appropriately adjusted.

The manipulator was a McFadden force loader system used in many aircraft research and development simulations. Three stick displacement configurations were employed. One was a fixed (no displacement) stick as in the F-16. The second had 0.77 deg/lb (small) stick motion. The third had 1.43 deg/lb (large) stick motion. The latter two matched the displacement/force characteristics employed in the NT-33 flight test. Analog signals from the manipulator force sensor (p_c) and the resulting

controlled element roll response ϕ were passed through an A → D converter to a digital computer where Y_pY_c describing functions and various performance measures were computed using STI's Frequency Domain Analysis (FREDA) program. The computations were essentially on-line and printed out at the conclusion of each run. Some 530 data runs were accomplished which provided a tremendous data base from which to determine or identify the various interactions of interest.

A key factor in the experimental program was that describing function measurements must cover the limb neuromuscular peaking frequency region, and forcing functions should be adjusted to emphasize good data in the neuromuscular subsystem region. Therefore, the initial forcing function was the sum of 8 sine waves ranging in frequency from 0.7 to 28 rad/sec. Example Y_pY_c describing function amplitude and phase data points for a K/s controlled element and fixed displacement force sidestick manipulator configuration are shown in Fig. 11. The data points reflect the frequencies used in the summation of sine waves.

The Bode amplitude plot shows that Y_pY_c is indeed ω_c/s-like in the region of crossover and there is a slight peaking (data points above the amplitude asymptote) in the region of 10-20 rad. Thus a first approximation to the data of Fig. 11 is the crossover model form which, as expected, works very well in the crossover region. A more refined amplitude and phase fitting program was then employed to identify fine-grained details in the dynamic model form and to extract parameter values. The resulting transfer function is illustrated in Fig. 11. The dashed lines represent the Bode asymptotes and the solid line the amplitude and phase for this transfer function. The resulting pilot model (Y_p) contains a low frequency first-order lag-lead, a first-order lag at 10 radians, a second-order lag with a frequency of 15 radians and damping ratio of approximately 0.4, and a high frequency lead at 8 rad/sec. The low frequency lag-lead slightly improves the very low frequency response, although they hardly matter here. The lags at 10 and 15 rad/sec are from the pilot's neuromuscular system. The lead at 8 radians is the usual adjustable pilot lead equalization. It is adjusted by the pilot here to offset some of the neuromuscular system lag. The pilot

ORIGINAL PAGE IS
OF POOR QUALITY

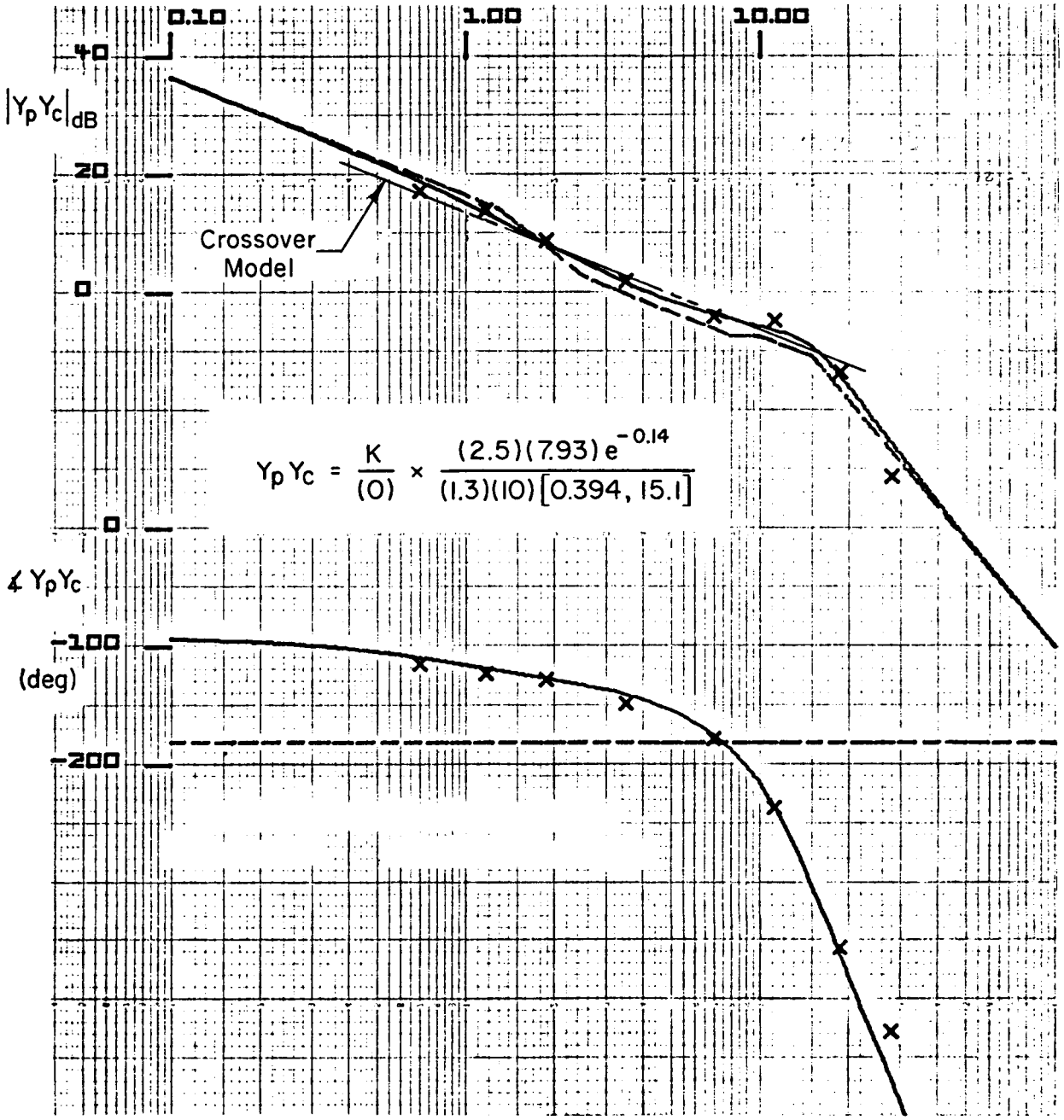

Figure 11. Example Describing Function Measurements and Extracted Parameter Values

model still includes an $e^{-\tau s}$, but in this case the τ is 0.14 instead of the usual 0.3 or 0.35 because it no longer encompasses the neuromuscular system contribution.

On the basis of such preliminary runs it was decided to move the input frequency at 28 rad/sec down to approximately 15 rad/sec in order to provide more data points in the vicinity of anticipated neuromuscular system peaking. Also another low frequency sine wave was added at about 0.46 rad/sec in order to require the pilot to hold forces for a longer period of time and hopefully further induce ratcheting. The final experimental runs were then accomplished using the summation of sine waves presented in Table 1.

TABLE 1. ROLL TRACKING FORCING FUNCTION

Sine Wave (i)	1	2	3	4	5	6	7	8	9
Frequency (ω_i)	0.467	0.701	1.17	1.87	3.51	7.01	11.2	14.0	18.7
Amplitude (A_i)	15.2	15.2	15.2	7.6	3.04	0.76	0.38	0.228	0.152
Relative Amplitude	1	1	1	0.5	0.2	0.05	0.025	0.015	0.01

$$\phi_I = \Sigma A_i \cos \omega_i t \quad \text{(deg)}$$

SECTION IV

EXPERIMENTAL RESULTS

RESULTS CONNECTED WITH THE CROSSOVER MODEL

It will be recalled that in the ideal crossover model the crossover frequency remains constant even though the controlled element gain may vary. Figure 12 shows results obtained using the fixed side-stick manipulator configuration and a wide range of command/force gradients (controlled element gains). The initial command/force gradients for the F-16 and the NT-33 experimental programs are identified for comparison. The controlled element forms range from K/s to $Ke^{-0.07s}/s(0.1\ s + 1)$. The data for various time delay or time lags are indicated by the symbols. The data points of Fig. 12 indicate two aspects. First they reflect a general decrease in ω_c as controlled element lags increase. Second they show that crossover frequency, as expected, is essentially independent of controlled element gain over a very broad region. But, as the controlled element gain becomes quite low and the manipulator forces required to achieve the desired rolling response become very large, a point is reached where the pilot can no longer accommodate and a rapid drop off in bandwidth results. Interestingly, the F-16 command/force gradients for both the production and the modified force stick characteristics lie right at the break in ω_c and therefore represent the lowest values which might be considered acceptable to pilots.

The rules associated with the ideal crossover model also state that for a given controlled element the pilot will adjust his gain such that the product of the crossover frequency ω_c and the rms tracking error remain constant across all controlled element gains. This premise is tested in Fig. 13 which plots $\omega_c\sigma_e$ vs. controlled element gain. Unfortunately a consistent set of data for this performance measure was only obtained for command/force gradients between 7.5 deg/sec/lb and 20 deg/sec/lb. This is the region for which the crossover remained relatively constant in Fig. 12 and the results in Fig. 13 show that the performance

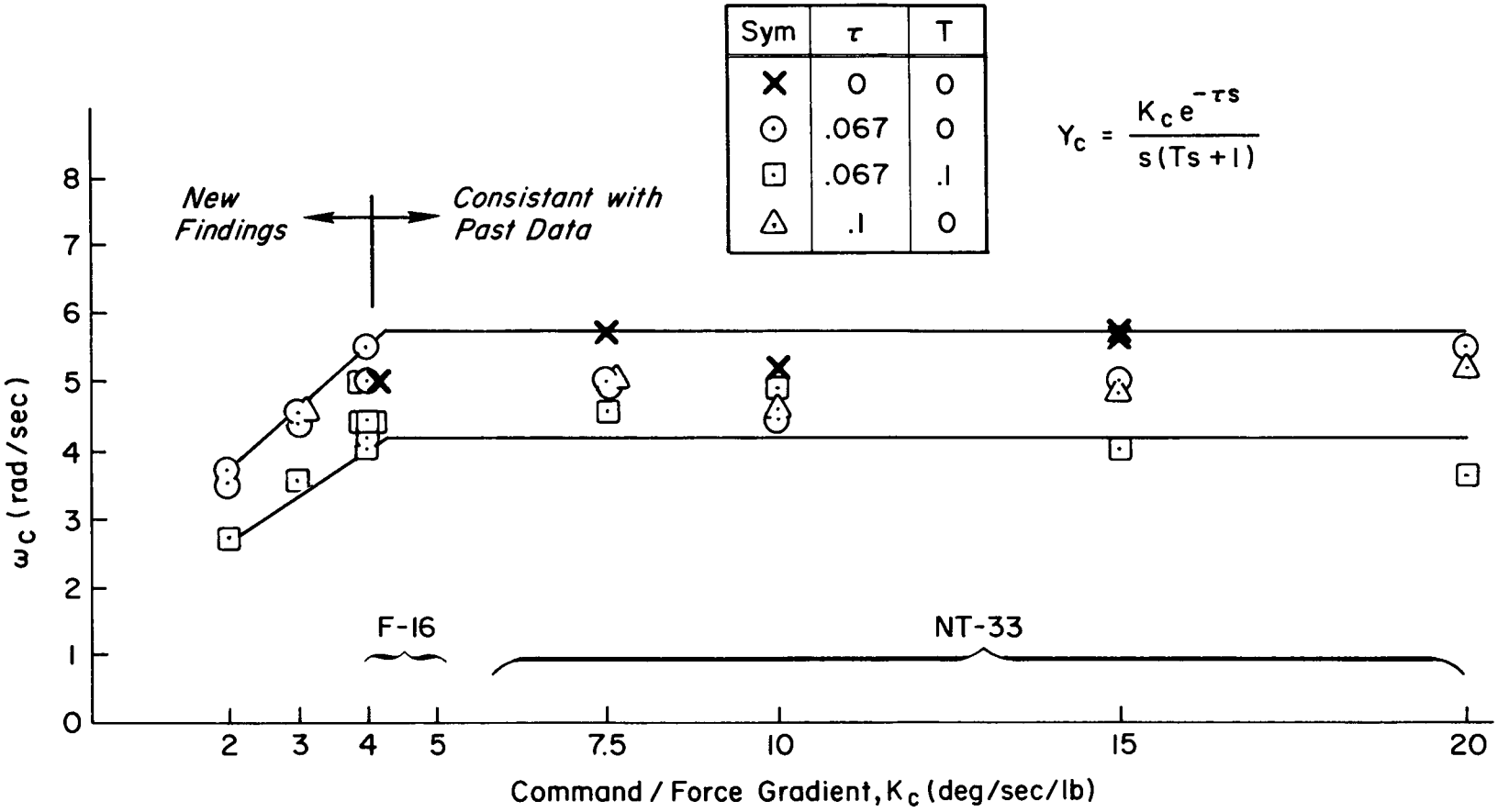

Figure 12. Influence of Command/Force Gradient on Crossover (Fixed Stick)

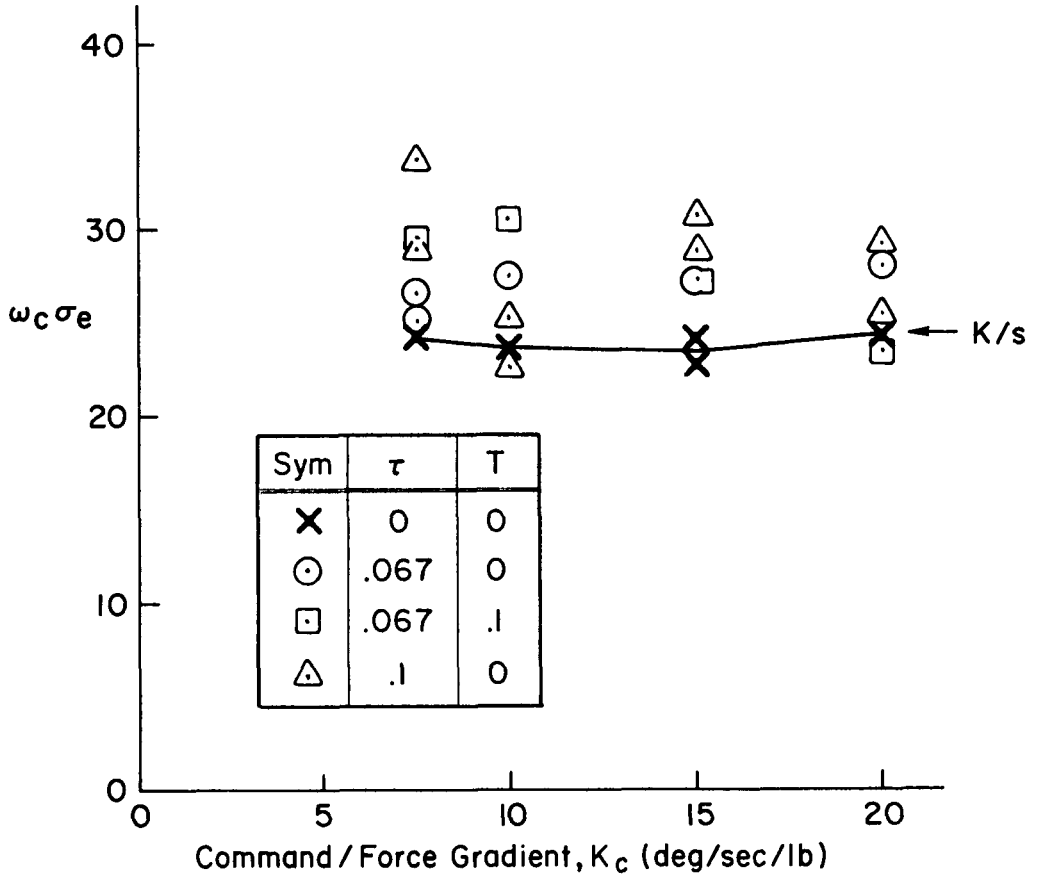

Figure 13. Influence of Controlled Element on Crossover Model Performance Metric (Fixed Stick)

measures remain within a relatively narrow band. For the baseline K/s controlled element the performance metric is essentially constant. For the other configurations which include time delay and/or prefilter lag, there is some scatter; however, the performance measures stayed quite consistant for each set of dynamics.

Plots of crossover frequency vs. command/force gradient for the small and large displacement side-stick controllers are shown in Fig. 14. For the small displacement stick the region where the crossover frequency remains essentially constant only extends from 10 to 20 deg/sec/lb. For controlled element gains less than this there is again a steady decrease in bandwidth achievable. The lower range of

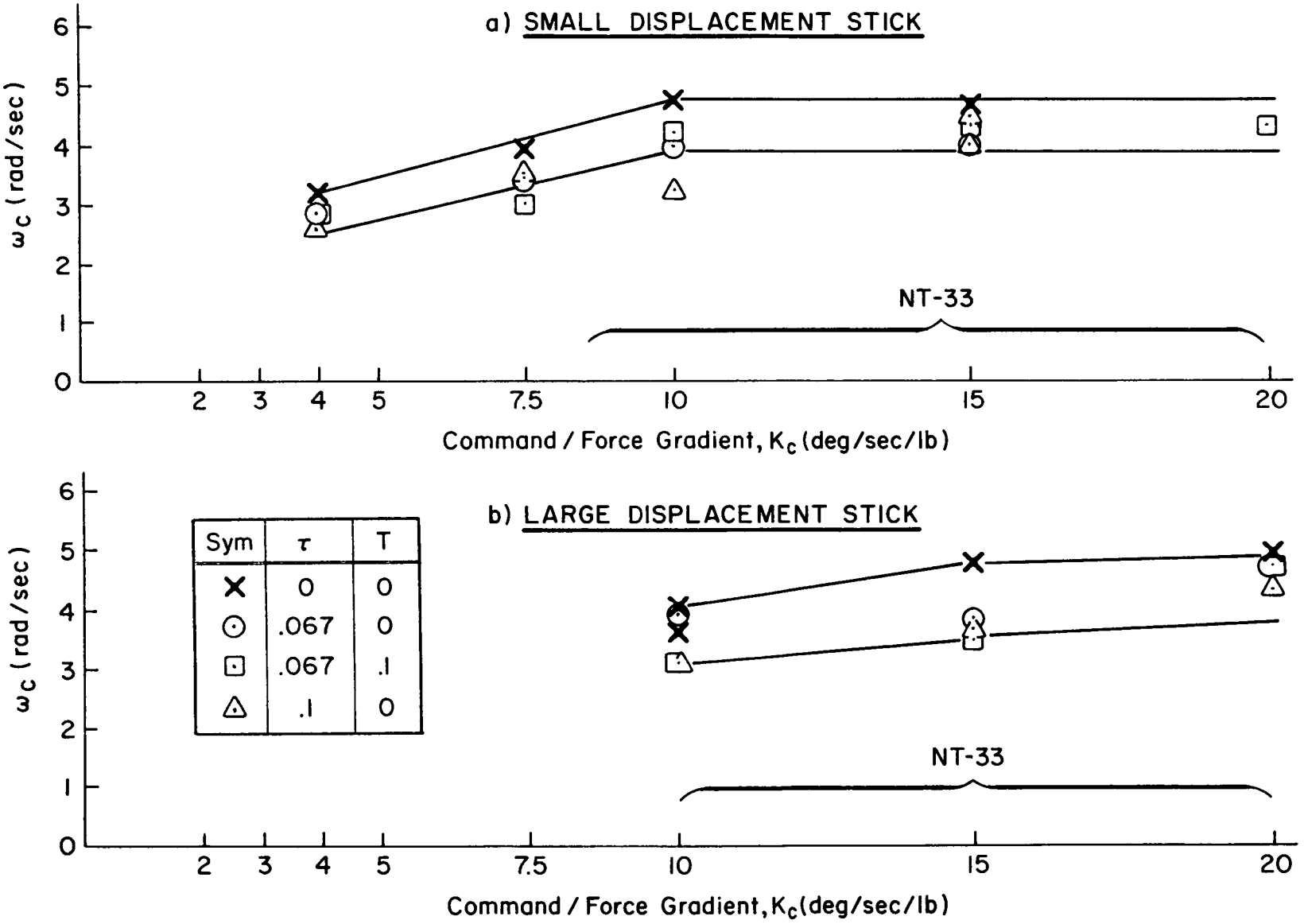

Figure 14. Influence of Command/Force Gradient on Crossover

controlled element gains were not investigated with the large displacement stick because the combination of large forces and large displacements made tracking almost impossible. However, at the higher controlled element gains there is no significant difference from the small displacement stick. Comparison of Figs. 12 and 14 shows there is a steady reduction in ω_c as stick displacement is increased.

Figure 15 shows similar results to those of Fig. 13 in that the performance measure $\omega_c \sigma_e$ remains essentially independent of controlled element gain, phase lag, and manipulator displacement.

RESULTS ASSOCIATED WITH THE LIMB-MANIPULATOR-NEUROMUSCULAR SYSTEM

Turning attention now to the neuromuscular system, we are interested in the amplitude ratio peaking and the possibility that this peaking will be sufficiently high that it will be cut by the 0 dB crossover; thus producing a high frequency resonance which could affect roll ratchet. Figure 16 presents the describing function measurements for 3 runs using the fixed force stick and a controlled element having a command/force gradient of 4 deg/sec/lb, no time lag, and a time delay of about 70 ms. The straight line reflects the resulting ω_c/s crossover characteristics. Amplitude departures from this asymptote are the contributions of the pilot's neuromuscular system at high frequency and his trim lag-lead at low frequency. In the region of crossover $Y_p Y_c$ is almost exactly ω_c/s as suggested by the ideal crossover model. The amplitude ratio departures from the asymptote at the highest 3 frequencies shows a peaking in the vicinity of the 14 rad/sec forcing function for 2 of the 3 runs. It also might be noted that there is remarkable consistency in both the amplitude and phase measurements across all frequencies for all 3 runs. In Fig. 16, two of the amplitude data points at 14 rad/sec lie slightly above the 0 dB line. We would therefore expect this to represent a neutral or slightly unstable dynamic mode if the phase angle were near -180 deg at this frequency. This then could be interpreted as affecting roll ratchet.

The two data points at 14 rad/sec are 10 dB above the asymptote and may or may not be exactly the actual neuromuscular system peak, i.e.,

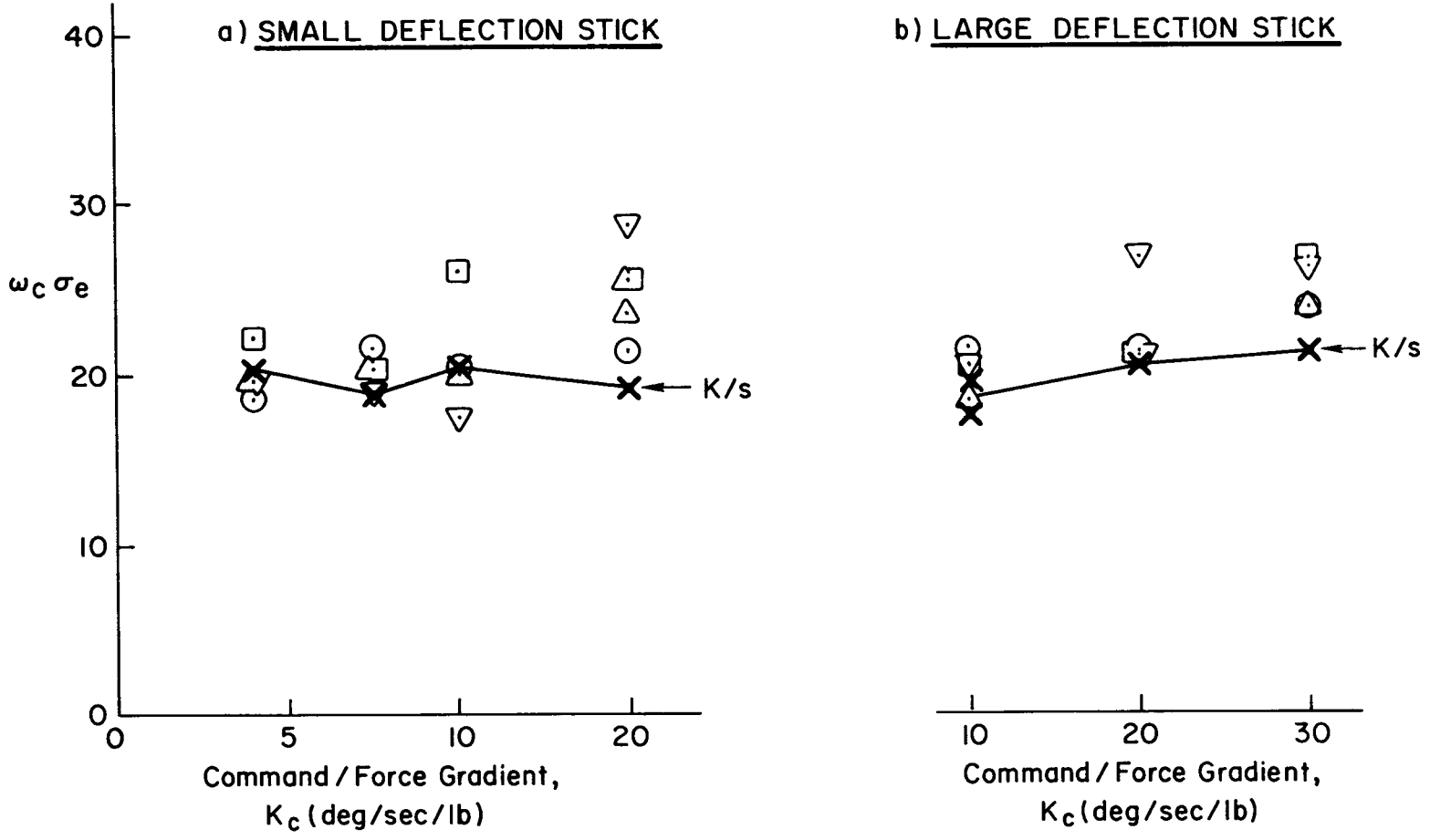

Figure 15. Influence of Controlled Element Gain and Stick Deflection on Crossover Model Performance Metric

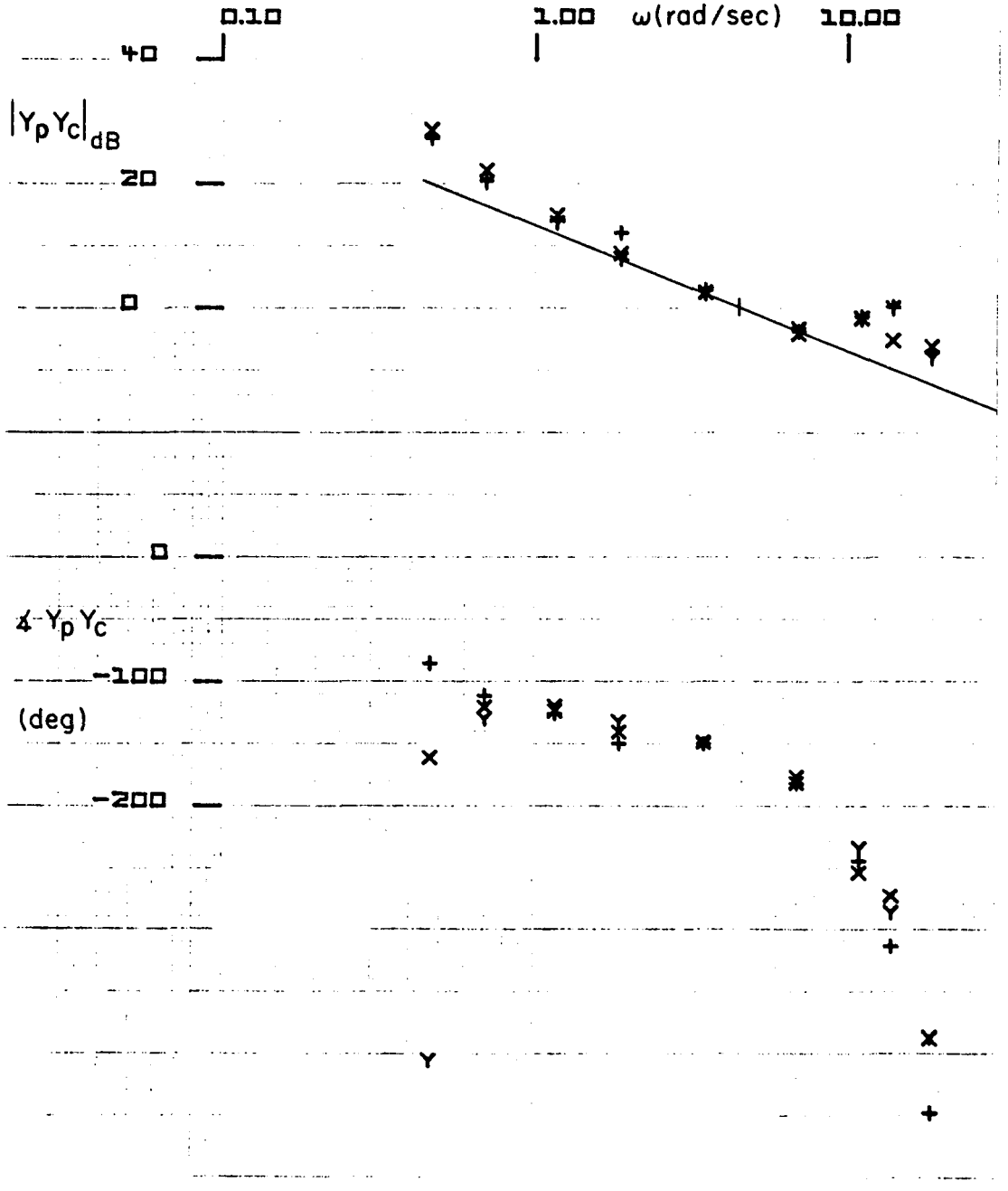

Figure 16. $Y_p Y_c$ Describing Function Amplitude and Phase Plot for $Y_c = 4/s\ e^{-0.067s}$

the peak itself may occur at a slightly higher or lower frequency. The peaking tendency shown in Fig. 16 is representative of a large amount of the data obtained. For example, the height of the amplitude data point above the K/s asymptote at the 3 highest frequencies from over 86 runs with the fixed stick is shown in Fig. 17. [The number of data points is not consistent across the three frequencies because run-to-run variability tends to increase at the highest frequencies and obviously wild data points have been thrown out.] The circles reflect the average values at each frequency and the bars indicate ±1 σ ranges.

All of these measurements were made with $\tau = 0.067$ and time lag time constants of 0 and 0.1 secs. Controlled element gains span the complete range shown in Fig. 12. The data consistently show the maximum departure to be detected at the 14 rad/sec input frequency. Again this may or may not be the actual peak of the neuromuscular system. Note that the average peaking across the 80 runs is approximately 8.5 dB at 14 rad/sec. This frequency is consistent with the roll ratchet frequencies observed in the flight traces.

The sensitivity of the 14 rad/sec peaking tendency to time delay is shown in Fig. 18. Here the controlled element is $K_c e^{-\tau s}/s$. The manipulator is again the fixed stick. As indicated in the figure, runs were made with the τ of 0.0, 0.05, 0.067, 0.08, and 0.1 secs. Results show that a time delay of approximately 0.065 to 0.07 tends to maximize the neuromuscular system peaking. At time delays either below or above these values, the peaking tendency decreases. Of all the controlled elements examined here K_c/s shows the minimum tendency for a peak. Interestingly, the time delay values which maximize the neuromuscular peaking would be considered good from the MIL-8785 flying quality specification standpoint. In essence, these data show that the tendency to peaking can be "tuned" by the adjustment of the controlled element effective lag, with a maximum effect near 0.07 sec.

The neuromuscular system peaking sensitivity to controlled element command/force gradient is shown in Fig. 19. Here the command/force gradient ranges from 3 deg/sec/lb (which is slightly lower than that employed on the F-16) up through 15 deg/sec/lb which was utilized in the

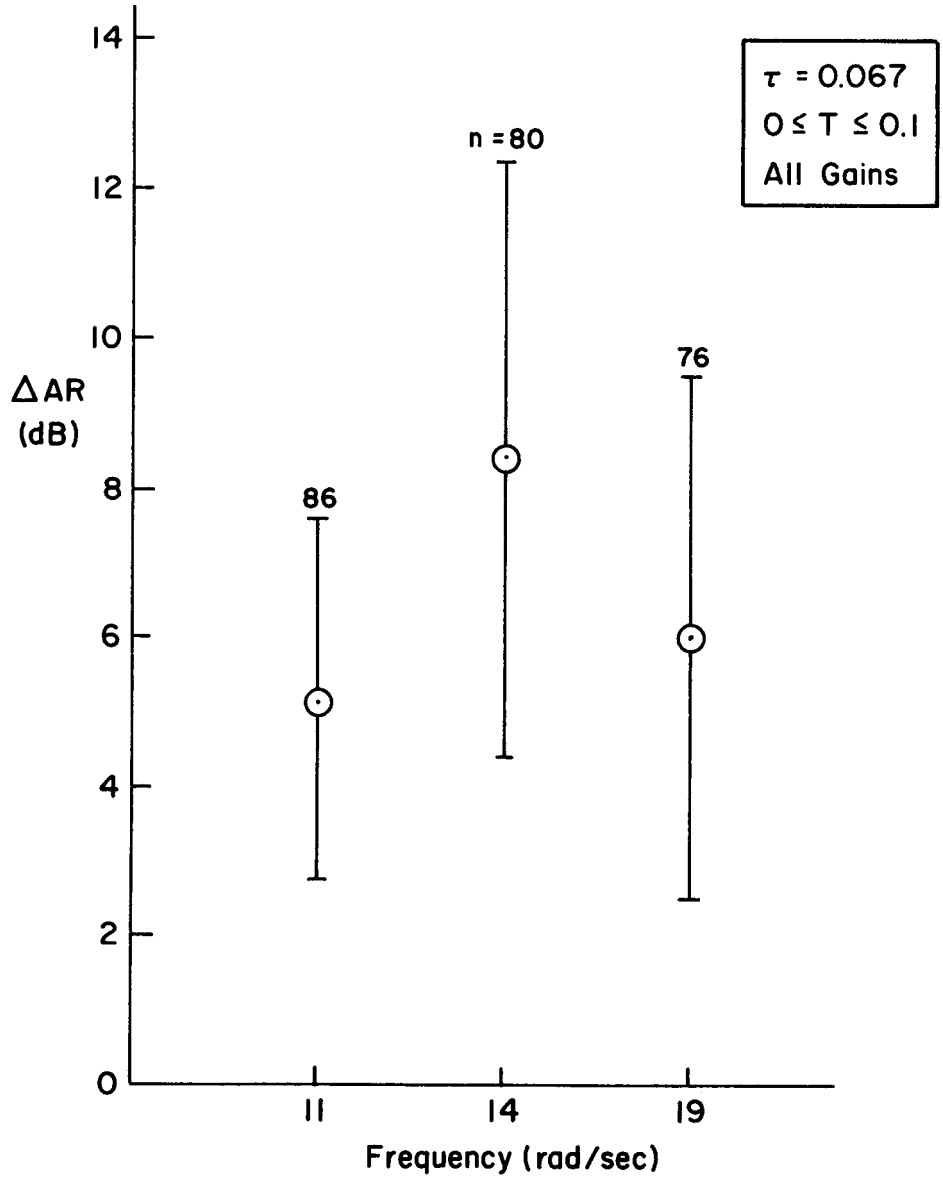

Figure 17. Neuromuscular System Amplitude Ratio Departure From Bode Asymptote (Fixed Stick)

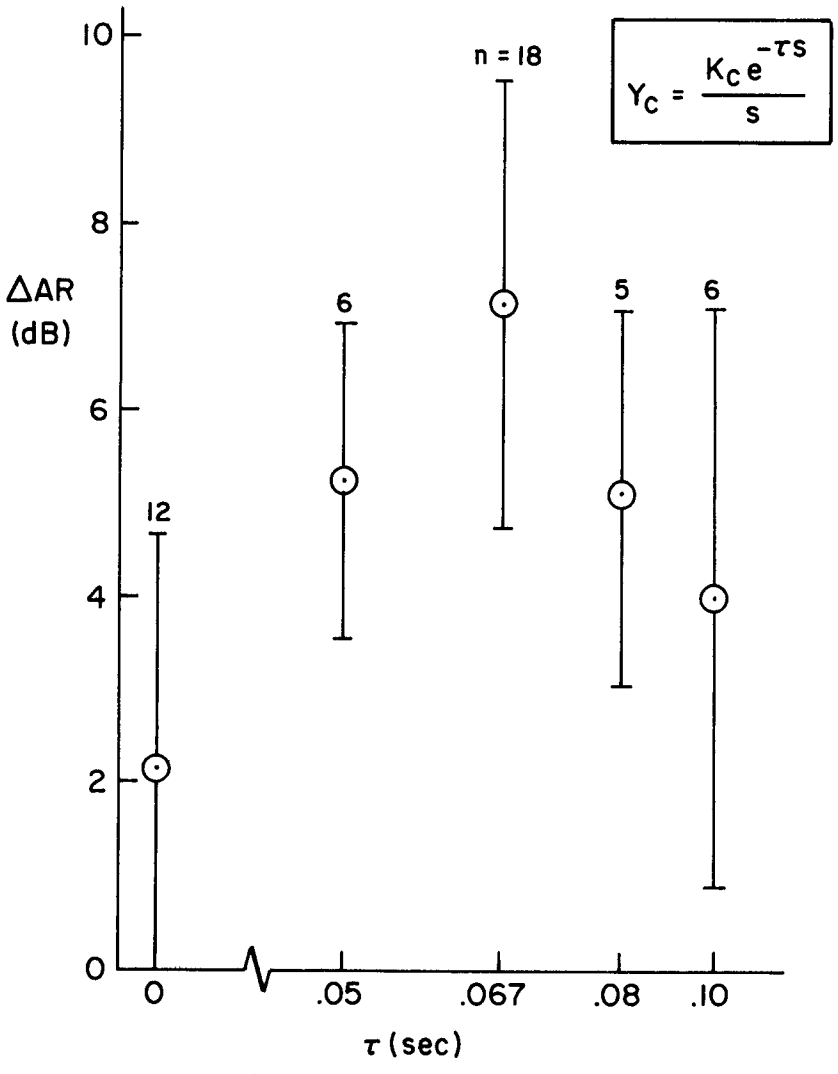

Figure 18. Neuromuscular System Amplitude Ratio Peaking With Controlled Element Time Delay (Fixed Stick)

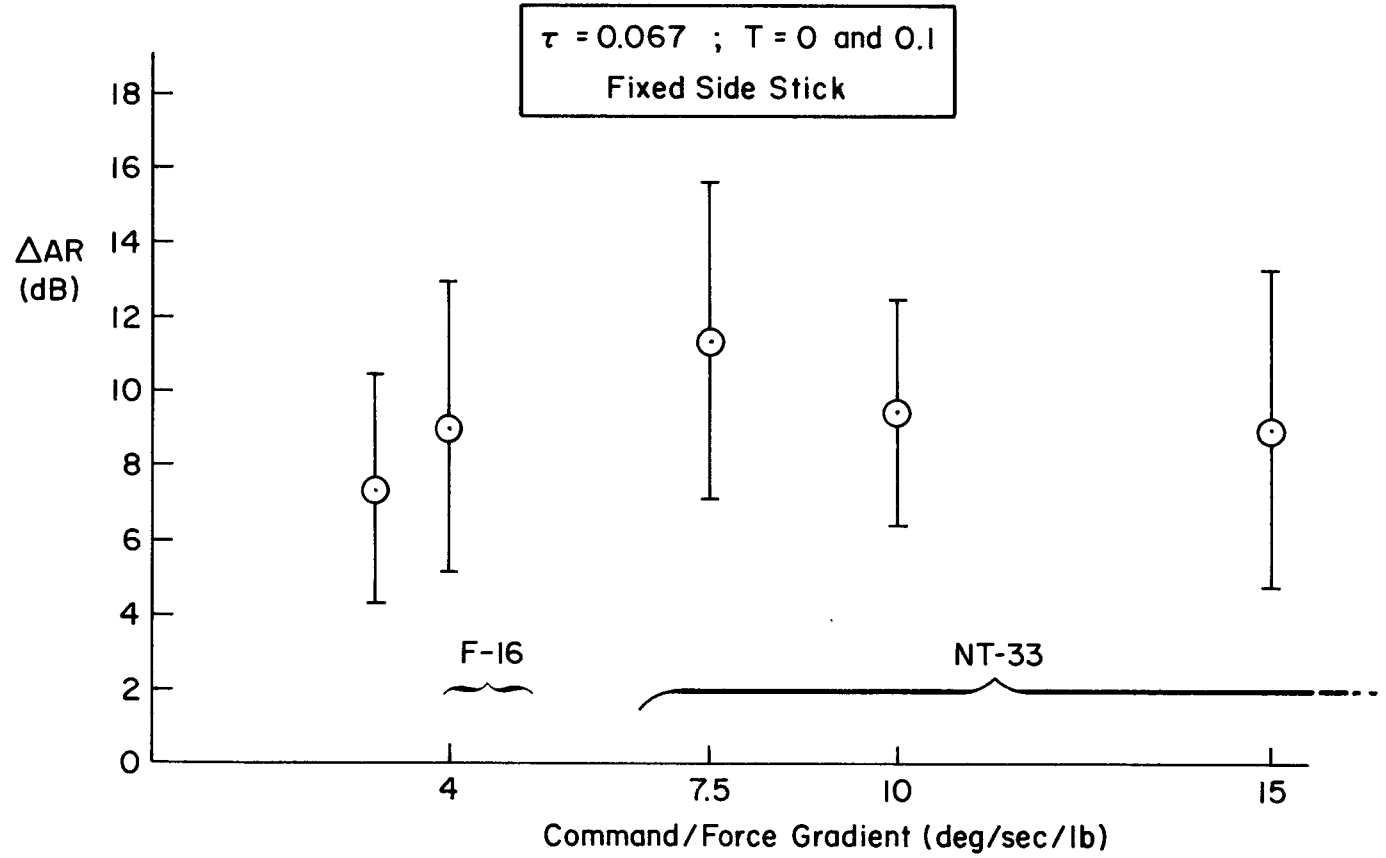

Figure 19. Neuromuscular Peaking Sensitivity to Controlled Element Command/Force Gradient

NT-33. The data were obtained using the fixed stick and a time delay of 0.067 sec which was selected because it yielded maximum peaking in Fig. 18. Data for time lags of 0 and 0.1 have been combined. These data show a slight peaking tendency in the vicinity of 7.5 deg/sec/lb command/force gradient. This is about the same value as the response/force ratio for the Fig. 1 flight traces of ratchet. This may or may not be coincidental. However, it is significant that there is appreciable peaking of the neuromuscular system across the entire gain range investigated in these experiments.

The influence of stick motion is summarized in Fig. 20. These plots reflect the amplitude ratio peaking at the 3 higher frequencies (11, 14, and 19 rad/sec) for the fixed, the small deflection, and the large deflection stick configurations at 3 different values of the controlled element time delay: 0.0, 0.067, and 0.1 secs. All of these data were taken with the command/force gradient of 10 deg/sec/lb, which is the medium initial command/force gradient in Fig. 8 for air-to-air tracking and about equal to the second command/force gradient for the production F-16 in gross maneuvering as shown in Fig. 9. The results in Fig. 20 show that there is relatively little difference between the fixed and small deflection force stick. Both show an increase in neuromuscular peaking tendency for the 0.067 and 0.1 sec time delays. They both show a tendency to maximum peaking in the vicinity of 14 rad/sec. In both cases there is considerably less peaking for the zero time delay cases although there may be some argument for the neuromuscular system peak to be occurring at 19 rad/sec (or higher) with zero time delay and the fixed stick. The large deflection stick, on the other hand, shows a relatively constant amplitude departure from the controlled element asymptote across the 11 to 19 rad/sec frequency band and a lack of sensitivity to the controlled element time delay. The reason for the reduced peaking with the large deflection stick is not fully established at this point; however, it may be related to the reduced crossover frequency which this stick induced (see Figs. 12 and 14). Figure 12 shows the bandwidth achieved with the fixed force stick was generally in the

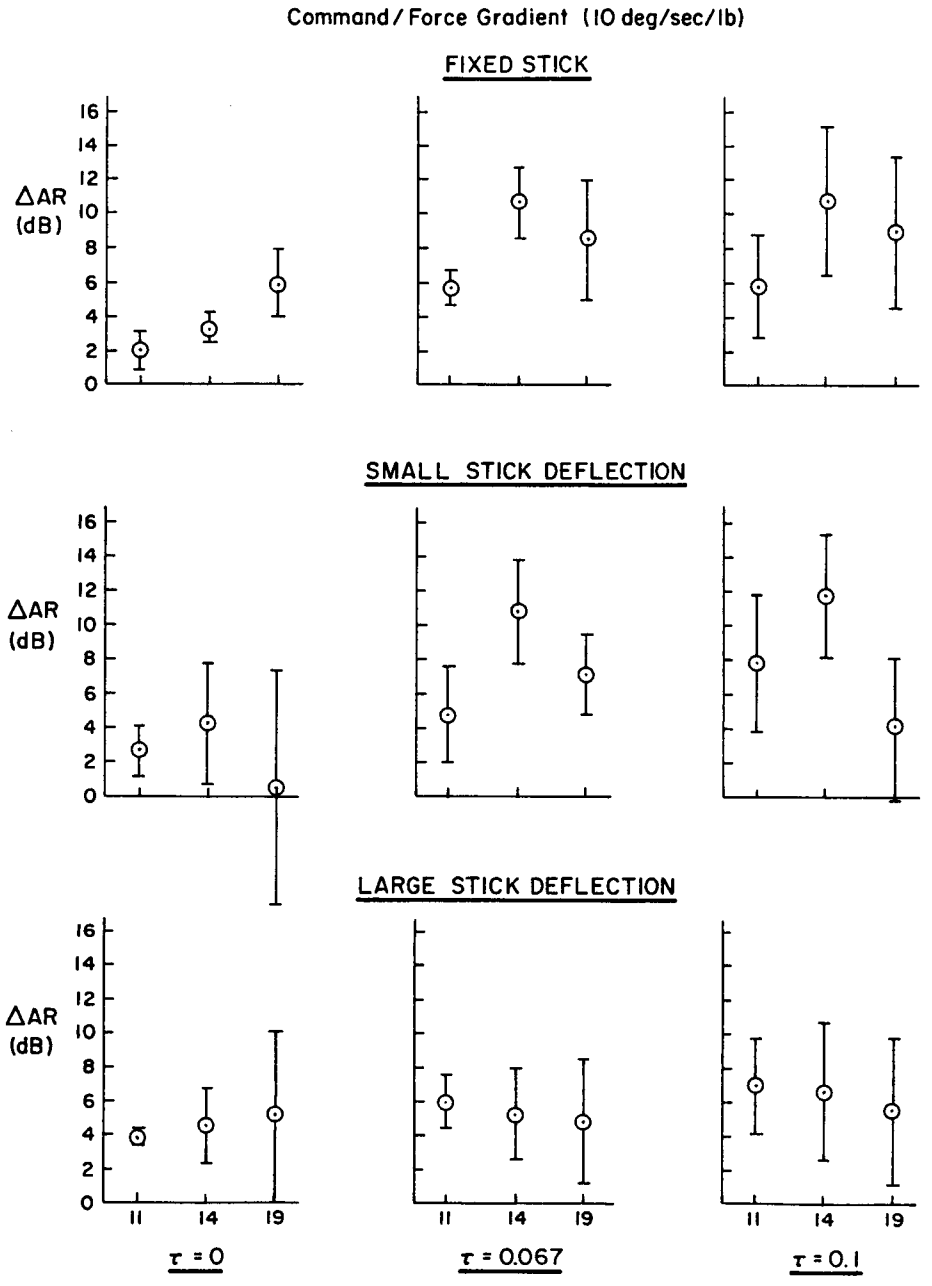

Figure 20. Influence of Stick Displacement on Neuromuscular Peaking Tendency

region of 4 to 6 rad/sec while Fig. 14 shows that for the large displacement stick the bandwidth was in the range of 3 to 5 rad/sec. This trend is consistent with the physiological system and effective pilot neuromuscular system time delay differences described in Section II.

The influence of the lag time constant on the neuromuscular system peaking and the possible adoption of lead by the pilot is reflected in Figs. 16 and 21 through 23. Figure 16 shows the neuromuscular peaking obtained with the controlled element command/force gradient of 4 deg/sec/lb and a time delay of 0.067 secs. The maximum peaking was noted to be approximately 10 dB and occurred at 14 rad/sec. The addition of a first-order lag time constant of 0.1 sec is shown in Fig. 21. Here the solid line represents the controlled element (Y_c) Bode asymptote adjusted to go through ω_c. The crossover occurs in a region that is K/s in appearance, and the amplitude peaking again is approximately 10 dB, and occurs near the 14 rad/sec data point. The peaks are quite close to the 0 dB gain line, which indicates a likely tendency to roll ratchet. Comparison of the phase plots between Figs. 16 and 21 indicate that the pilot is generating little if any lead to offset the time lag.

In Fig. 22 the time lag has been moved to 0.2 secs. Comparison of the phase angle data points in Figs. 16 and 22, or Figs. 21 and 22, indicate that the pilot has introduced lead in the Fig. 22 case which essentially cancels the time lag at 0.2 secs. The asymptote for the Y_pY_c open-loop system is thus represented by the solid line below the time break point and the dashed line above that break point. Again the amplitude ratio is ω_c/s-like in the vicinity of the crossover. However, there is now considerable scatter in the data points in the region of the neuromuscular system peaking dynamics. In only one of the three runs shown in Fig. 22 was there a peaking tendency for the neuromuscular system and this appears to be concentrated in the vicinity of 11 rad/sec rather than the 14 as noted previously. In the other two runs, the amplitude data points lie quite closely to the Y_pY_c asymptote.

Comparison of the data for T = 0, 0.1, and T = 0.2 sec (e.g., Figs. 16, 21, and 22) provide basic information about pilot lead generation. The crossover model implies that a first-order controlled element

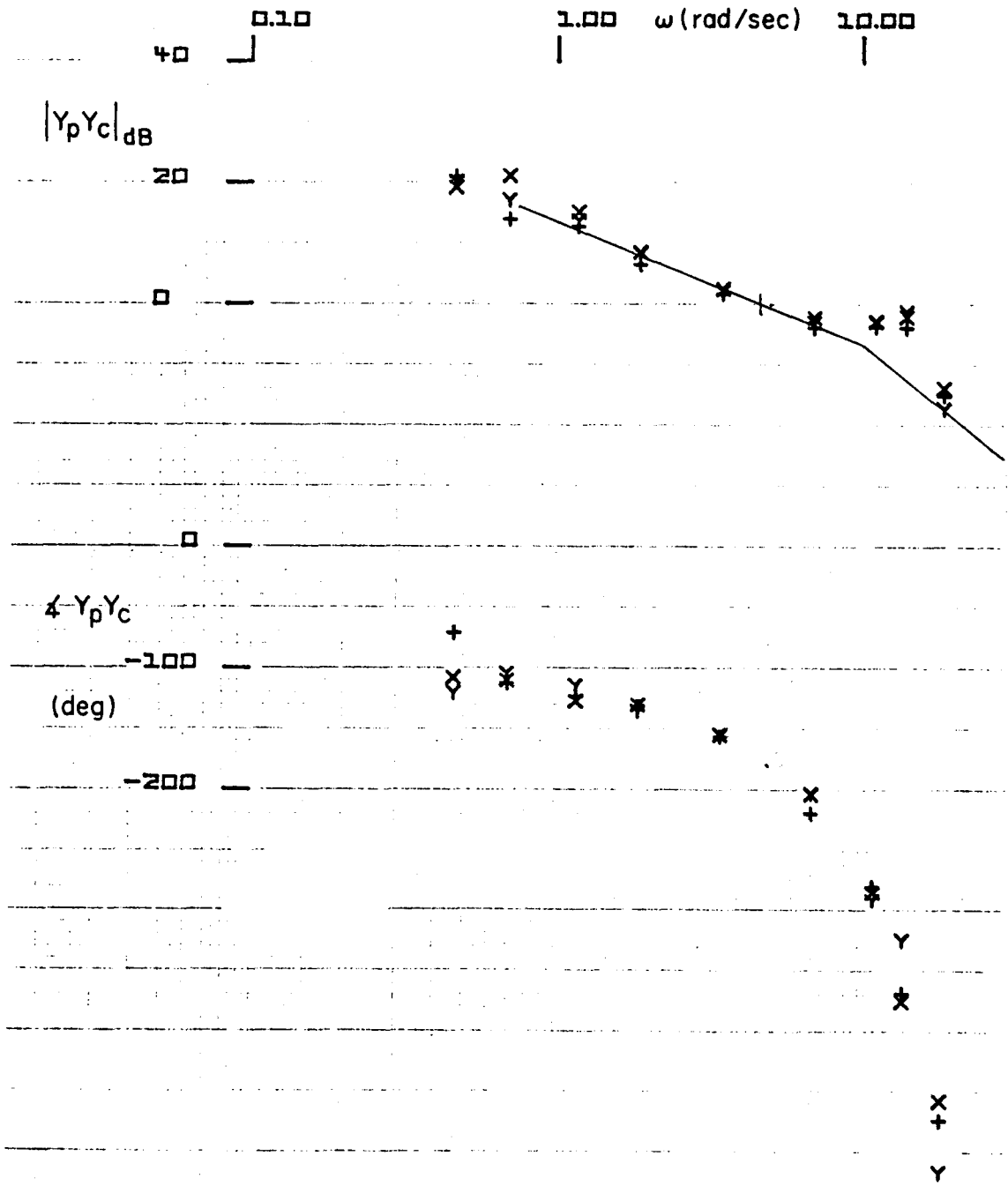

Figure 21. Y_pY_c Describing Function Amplitude and Phase Plot

For $Y_c = \frac{4e^{-0.067s}}{s(0.1s+1)}$

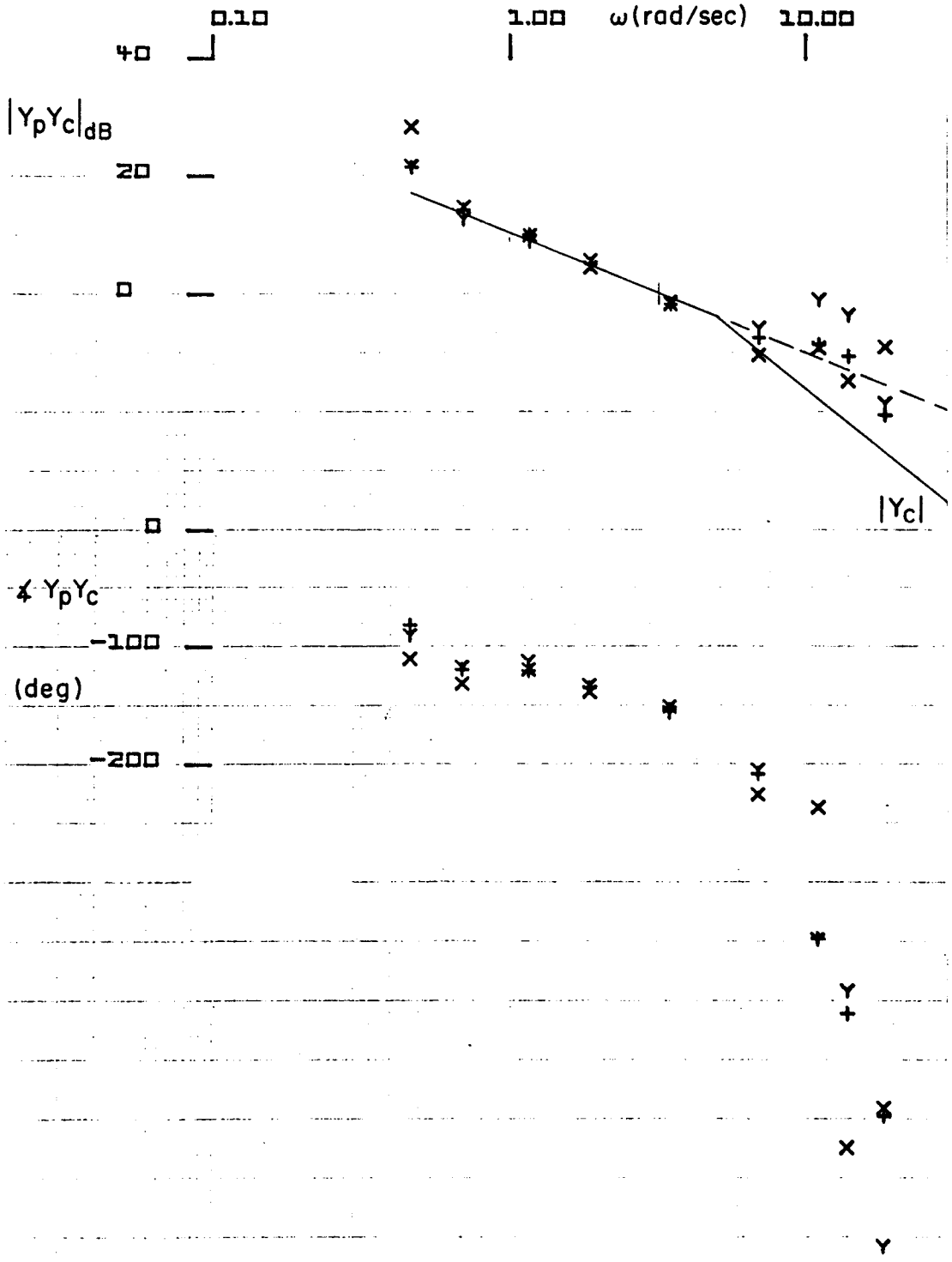

Figure 22. Y_pY_c Describing Function Amplitude and Phase Plot

For $Y_c = \frac{4e^{-0.067s}}{s(0.2s+1)}$

lag in the region of crossover is compensated for by a pilot lead. In the absence of any such lag the pilot lead is adjusted to offset neuromuscular delays, as exemplified by the lead at 8 rad/sec in Fig. 11. Nearly the same result applies for a controlled element lag of T = 0.1 sec. Then, for T > 0.2 sec the pilot lead, T_L, is adjusted to compensate, i.e., $T_L \doteq T$.

In Fig. 23 the lag time constant has been moved down to 0.4 sec. Again comparison of the phase plots shows that the pilot has now moved his lead down to precisely cancel the controlled element time lag contribution so that the resulting Y_pY_c has the appearance of an ω_c/s throughout the frequency region of interest. The peaking tendency of the neuromuscular system is no longer evident and there should be little chance of roll ratchet. However, the roll control bandwidth has now been reduced to approximately 2.5 rad/sec whereas it was approximately 4.5 rad/sec with the time constant of 0.1 sec. If the pilot were to attempt to achieve a 4.5 rad/sec bandwidth in the presence of the lag characteristics shown in Fig. 23, a PIO would occur at roughly that frequency (4 rad/sec). Thus in reducing or eliminating the roll ratchet tendency, we may have substituted a tendency for the lower frequency PIO.

EXTRAPOLATION OF FIXED-BASE DESCRIBING FUNCTION RESULTS TO ESTIMATES FOR FLIGHT

The previous sections have emphasized the neuromuscular peaking tendency as a harbinger of the roll ratchet phenomenon. Yet, in the data presented, the open-loop system phase angle has generally been greater in magnitude than -180 degrees. This means that the gain differences between the peak and the 0 dB line are not necessarily true gain margins. The closed-loop pilot-vehicle systems will, therefore, not necessarily show an oscillation at the neuromuscular peaking frequency although the resonant peak will ordinarily be indicated in the closed-loop system. The pilot remnant, being relatively broadband in character, will therefore act as a driving mechanism to excite the resonant peak.

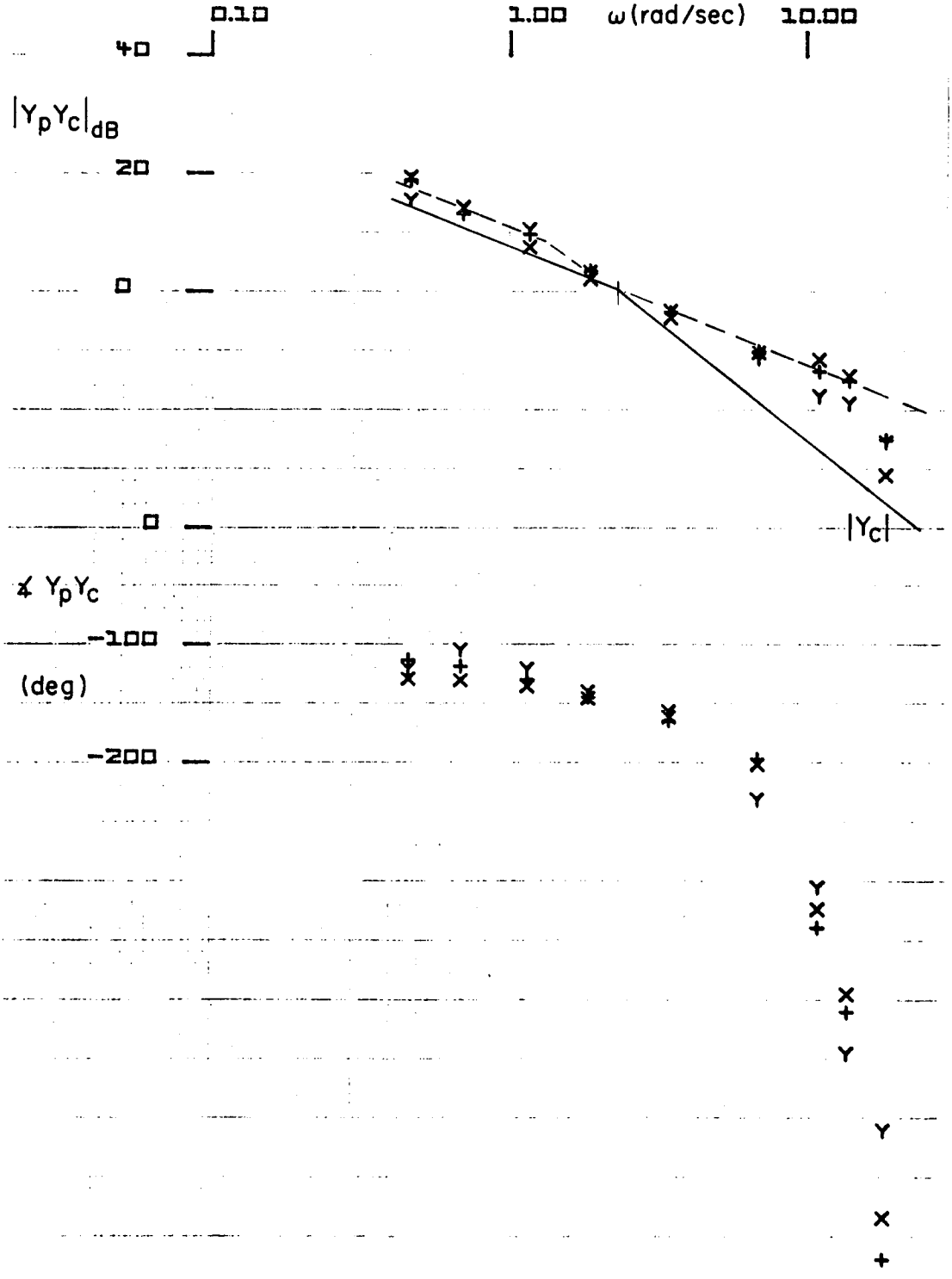

Figure 23. Y_pY_c Describing Function Amplitude and Phase Plot

For $Y_c = \frac{4e^{-0.067s}}{s(0.4s+1)}$

In some cases the experimental data actually indicated a roll ratchet-like oscillation under conditions similar to those where the phenomenon was found in flight. Most commonly these were stretches in the time histories which involved nearly steady-state rolling velocity commands. An excellent example is given in Fig. 24. Here a short segment of the roll attitude command input is nearly triangular, and the pilot's stick force trace indicates a 2-3 Hz oscillation. Because the forcing function is a random appearing time signal, with only very occasional segments akin to the triangular or steady rolling commands shown, this type of ratchet-like pilot output trace is atypical in the context of a total experimental run. The pilot subjects, in fact, did not report that they had encountered the condition since it was so transitory. Yet it appeared quite commonly once the conditions were favorable -- i.e., neuromuscular peaking tendency present and momentarily steady rolling velocity command. Consequently the fixed base simulation can be said to have successfully demonstrated roll ratchet-like phenomena.

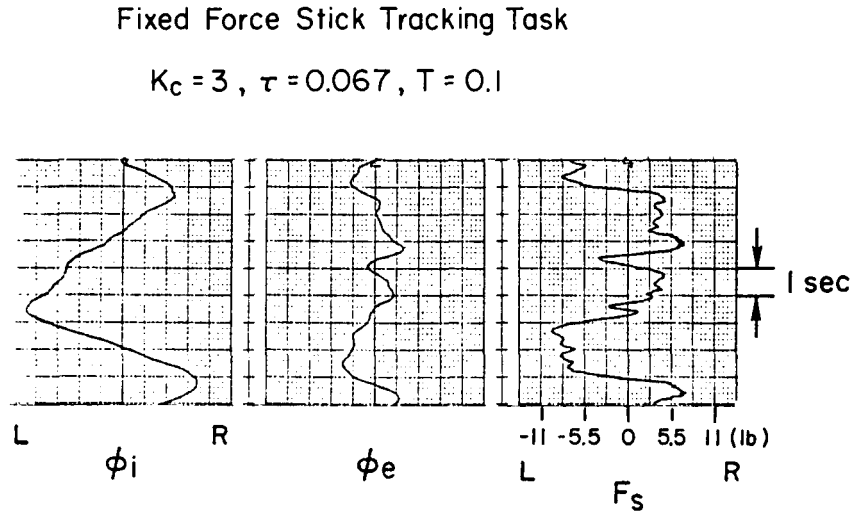

Figure 24. Example of Roll Ratchet-Like Oscillation in Stick Force Trace

It is also useful to re-examine the open-loop describing function data when a first-order correction is made to the data to account for rapid rolling motion. As summarized in Ref. 4, the pilot's angular motion sensing neurological apparatus acts very much like a rate gyro inner loop in the frequency range near and slightly above crossover. This inner loop, present when superthreshold rolling velocities are imposed on the pilot, has the effect of reducing the effective time lags in the pilot's visual-input/manipulator output response. The reduction can be as much as 0.1 second from the fixed-base data. When changes of phase lag of the magnitude 0.1 ω are made on typical describing function data showing major neuromuscular peaking, the net phase shift in the frequency region about the peak is very often near -180 degrees. Figure 25 shows two typical examples for the fixed force stick configuration with T = 0, τ = 0.067, and K_c = 10 and 15 deg/sec/lb. The solid line on the phase plot reflects the -180° phase line if a phase lag reduction of 0.1ω due to motion effects were included. These two cases reflect the F-16 gross maneuvering command/force gradients of Fig. 9. Therefore one can conclude that the fixed-base neuromuscular peaking examples which show negative gain margins of the amplitude ratio peak relative to 0 dB are quite likely to result in oscillations in the flight situation. The roll ratchet phenomenon in these cases would therefore be high-frequency PIO's which intimately involve the pilot's limb-manipulator neuromuscular system dynamics.

COMPARISONS WITH FLIGHT DATA

The controlled elements in Figs. 21-25 essentially duplicate the F-16 configurations tested in Ref. 14 and the qualitative results and trends are the same. The compromise selection for the prefilter in the F-16 (Ref. 14) was a time constant of 0.2 rad/sec. The Bode plot of Fig. 22 shows this allows a comfortable bandwidth slightly above 3 rad/sec and having 30 to 35 deg of phase margin and a much reduced neuromuscular peaking tendency. Thus there should be minimum tendency for either low or high frequency PIO although the data scatter in the higher frequency range of Fig. 22 show that conditions favorable to roll ratchet could pop up from time to time.

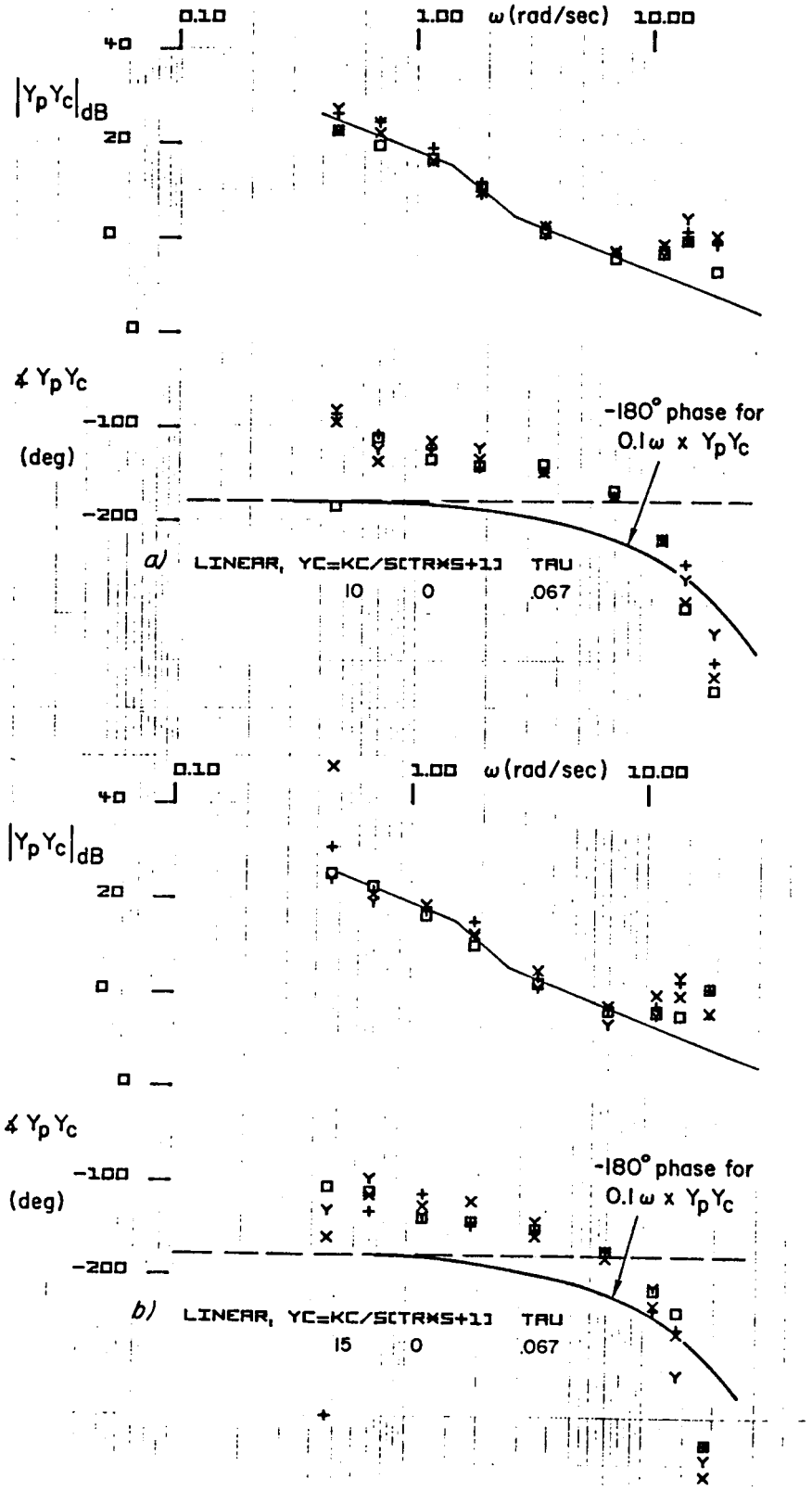

Figure 25. Expected Phase Shift Due to Motion Effects

Yet another comparison between simulation results and flight data can be drawn from the Ref. 6 investigation of roll ratchet and various prefilter configurations flown in the NT-33. In this case one set of effective controlled elements were of the form

$$\frac{\phi}{F_{AS}} = \frac{L'_{FAS}\, e^{-\tau s}}{s(s + 1/T_R)}$$

The parameters were varied over the ranges

$$0 < \tau < 0.105 \text{ sec}$$

$$0.15 < T_R < 0.8 \text{ sec}$$

$$10 < P_{SS}/F_{AS} < 25 \text{ deg/sec/\#}$$

and therefore are a close match to this simulation. A major difference, however, was the use of a center-stick in the NT-33.

The roll ratchet encountered in this flight test was described as "response which was objectionably abrupt, resulting in a very high frequency, pilot-induced-oscillation (wing rocking) or having 'square corners' or being very 'jerky.'" The frequency was approximately 16 rad/sec.

Figure 26 is a replot of data from Ref. 6 with command/force gradient plotted versus the roll time constant, T_R. The circles identify configurations flown; the open symbols reflect no ratchet obtained, the shaded symbols reflect roll ratchet observed by one or more of the evaluation pilots over the range of time delays investigated. (It should be noted in passing that in almost every case, the ratchet only occurred with non-zero τ as was the case in the lab simulation.) The numbers next to the circles are the average Cooper-Harper ratings given the configurations. Numbers on the left are ratings for up-and-away tasks; numbers on the right are ratings for landing tasks. The triangular symbol at $T_R = 0.2$, $K_c = 12.5$ is another NT-33 data point obtained from Ref. 16. It should be noted that in the Ref. 16 flight program the

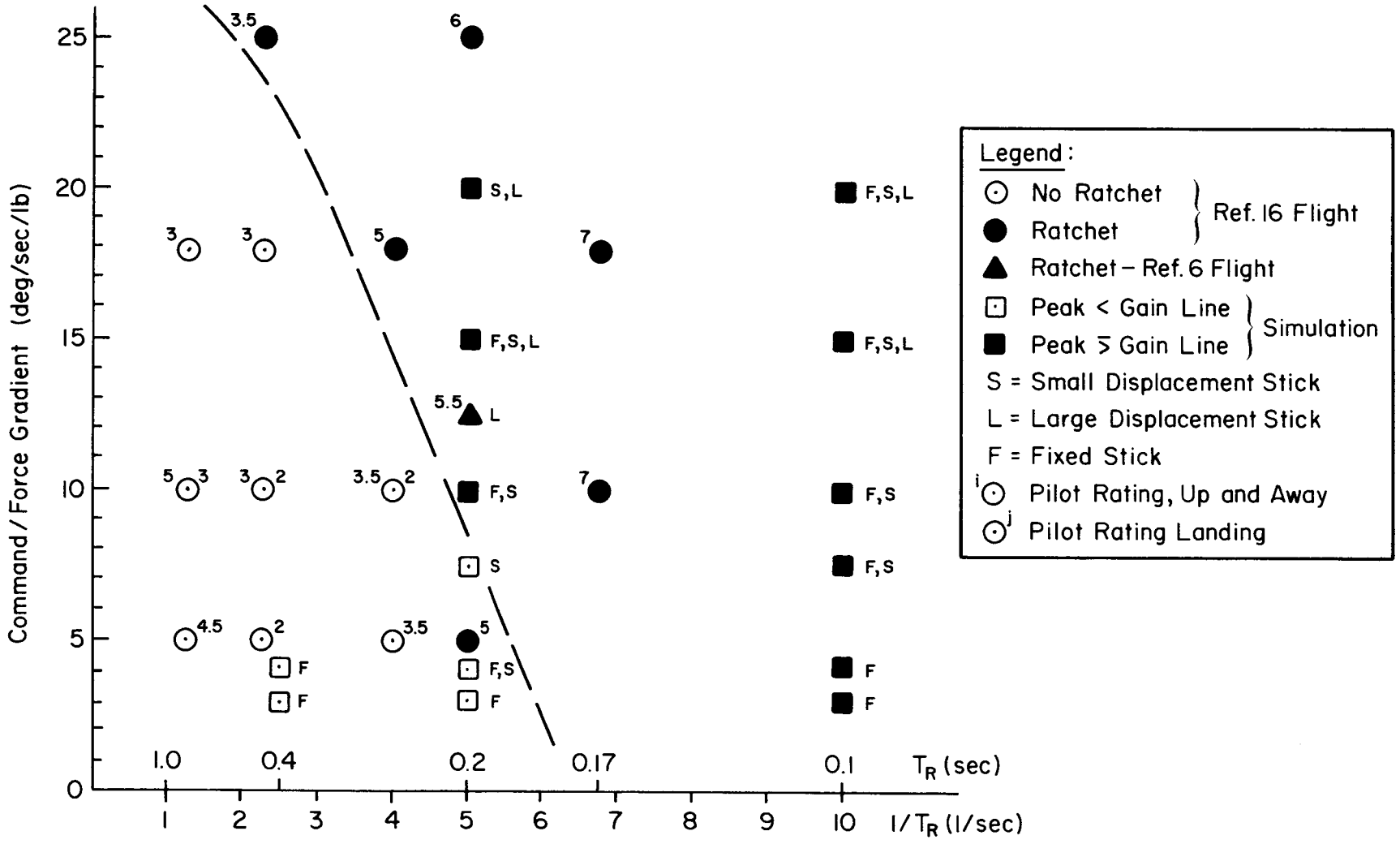

Figure 26. Roll Ratchet Comparison, Flight and Simulator

roll time constant was selected at 0.2 sec for up-and-away tasks and 0.5 sec for landing tasks. In addition, two 20 rad/sec first-order filters were included in the roll rate command prefilter to "eliminate high frequency noise." Even so, this one case of ratchet tendency was observed.

The square symbols in Fig. 26 are configurations investigated in the fixed-base simulation. The open symbols identify configurations for which the Y_pY_c zero dB line did not pass through the neuromuscular peak (no ratchet possibility). The shaded squares identify configurations for which the zero dB line passed through the peak (ratchet possibility). The letters F, S, L reflect the displacement of the simulator side-stick. It is likely that the L side-stick most closely matched the NT-33 center-stick characteristics.

There is very good correlation between the flight and lab simulation ratchet tendencies shown in Fig. 26. The dashed line appears to separate the non-ratchet from the ratchet configurations except for the two or three lowest command/force gradient configurations at T_R = 0.2 sec. It is possible that this difference may be related to wrist (simulation side-stick) versus arm (flight center-stick) neuromuscular subsystem contributions at the lower command (higher force) configurations. The good agreement between flight and simulator results is interpreted as an encouraging validation of the simulator definition of ratchet potential -- i.e., neuromuscular peaking cut by the Y_pY_c zero dB line.

PILOT-MANIPULATOR SYSTEM ASYMMETRIES

It was noted in the discussion of the influence of the command/force gradient on crossover in Fig. 12, that the control bandwidth ω_c decreased markedly as the command/force gradient decreased below 4 deg/sec/lb. The reason for this can be observed in the time traces of Fig. 27. The trace on the left is the random rolling motion of the target. The trace in the middle is the roll error between the target and the controlled element, the trace on the right is the stick force input to the controlled element. It will be noted on the force trace that in roll to the right the stick force rarely exceeds 5.5 lbs, but in

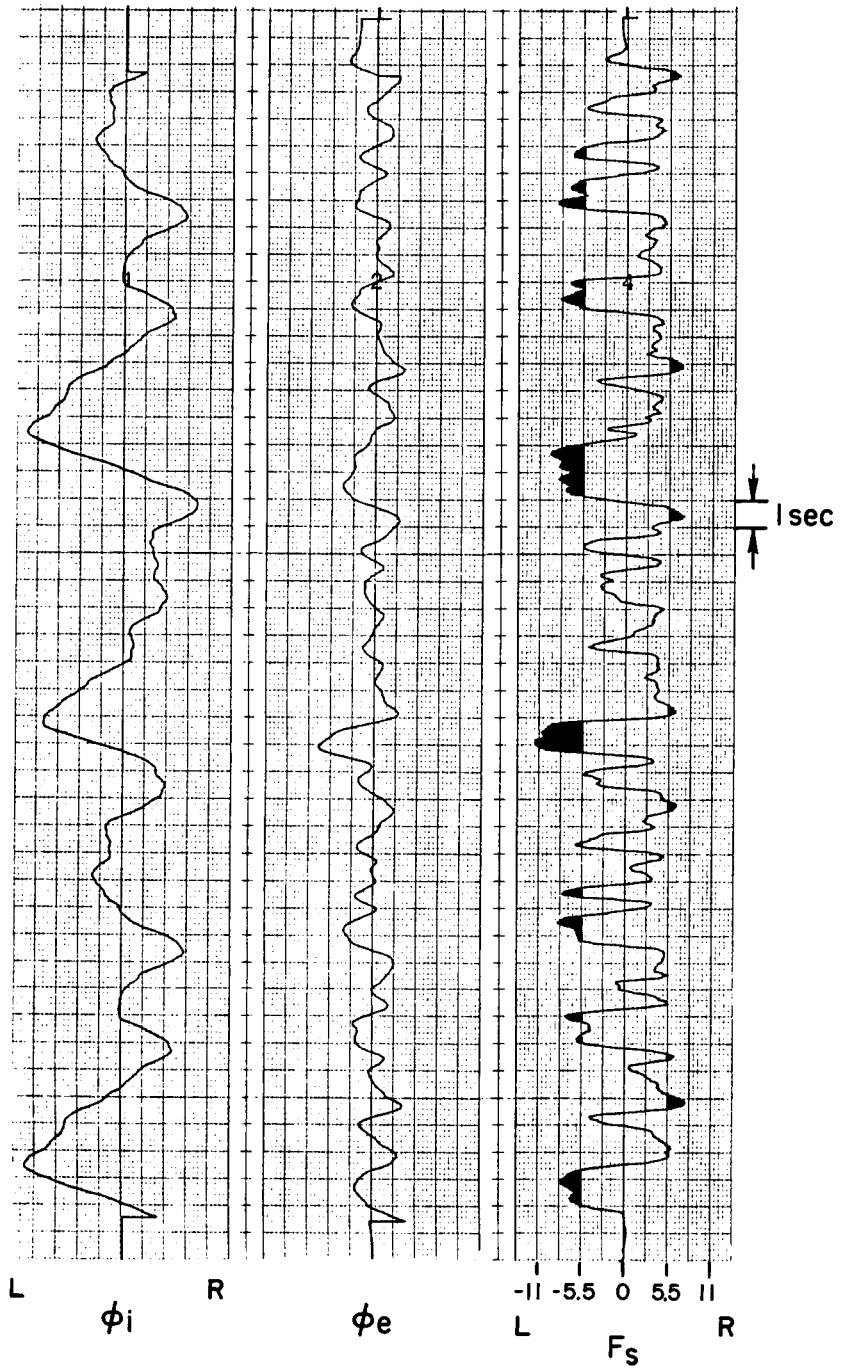

Figure 27. Time Traces of Fixed Force Stick Tracking Task
Run 115, K_c = 3, τ = 0.067, T = 0.1

rolls to the left the force frequently is as high as 8 lbs and shows a maximum peak at 11 lbs. This is consistent with the pilot commentary associated with Figs. 8 and 9 in which the pilots indicate difficulty in generating rolls to the right using the thumb, but have little difficulty in rolls to the left where they can use the entire palm of their hand to generate the force. Thus we see bi-modal control in the traces of Fig. 27 with larger magnitude, shorter duration forces in rolls to the left and lower magnitude, longer duration forces being used in rolls to the right. Notice that the roll error average is approximately zero in the middle trace. Thus the area under the force traces for left vs. right maneuvers must be approximately the same. For right rolls, lower forces are held for longer periods of time. This results in a lower crossover or bandwidth for right rolls as compared to left rolls and hence a lower average bandwidth for the run. This bi-modal control characteristic was most evident for the 3 deg/sec and 4 deg/sec/lb controlled element or command force gradients, but was also evident up as high as the 7.5 deg/sec/lb. Thus the reduced bandwidth shown in the Fig. 12 plots for the low gain systems. For higher command/force gradients, the forces employed in the tracking task were sufficently low that there was little difference between left and right maneuvers.

In conclusion, the results of this fixed-base experimental program have indicated that the neuromuscular system appears to be a large contributor to roll ratchet tendency. It was further shown that the neuromuscular peaking can be intensified by the use of fixed or small deflection force sticks, by having controlled elements with time delays in the vicinity of 60 to 70 ms, and by having time lags with time constants of 0.2 sec or less. Thus force sensing side-stick manipulators, prefilters, and flight control system time delays need to be carefully tuned in order to minimize neuromuscular peaking and consequent roll ratchet tendency and also to minimize restriction of roll control bandwidth and the tendency for low frequency PIO. The experimental results also demonstrated the problems in rolling to the right with fixed or small displacement side-sticks having high manipulator force gradients. In short, the simulation produced results consistent with all of the roll

control problems which have been reported in previous F-16 and NT-33 in-flight side-stick investigations. These results constitute a first step in defining design guides and criteria for manipulator and command augmentation system interfaces with the pilot. The results presented here reflect a mere skimming of the cream from these 530 simulation runs. Undoubtedly, the data archive contains much more information which can be gained from further and in-depth analysis of this data bank.

SECTION V

CONCLUSIONS

This fixed-base experimental investigation has identified and quantified interactions between the pilot's neuromuscular subsystem and such aspects of typical modern, high response, roll rate command control system mechanizations as:

- side-stick type manipulator force/displacement configuration
- command augmentation forward loop gain
- controlled element effective lag time constant
- flight control system effective time delay

The simulation results provide insight to high frequency roll ratchet oscillations, low frequency PIO, and roll-to-right control and handling problems previously reported in the production F-16, NT-33 side-stick, and NT-33 roll rate command augmentation investigations. The experimental configurations encompass and/or duplicate a number of actual flight situations and have reproduced control problems observed in flight. The data strongly support the suggestion that the roll ratchet phenomenon is a closed-loop pilot-vehicle interaction in which the pilots neuromuscular dynamics play a central role.

This is believed to be the first detailed investigation searching for roll ratchet tendencies in a ground based simulation (fixed- or moving-base). Detection of peaking tendencies was afforded by the use of a tight roll tracking task having a carefully tailored forcing function containing excitation frequencies covering the nominal range of the neuromuscular system mode and application of frequency response (FREDA) spectral analysis techniques. These procedures were particularly important because they allowed detection of the high frequency oscillatory (roll ratchet) tendency where small as well as large manipulator forces, and very small excitation and/or output signals, were involved. Such procedures are recommended as preflight development tests with modern

fly-by-wire command augmentation systems since, in this fixed-base simulation, at no time was ratchet tendency apparent to the subject pilot in the tracking display. Another aspect of the forcing function selection to help detect neuromuscular roll ratchet in time traces of the pilot's manipulator force/roll rate command signal is the tracking task scenario. This must be structured so that the pilot is required to hold moderate to high constant force levels for several seconds duration. These procedures can serve as a basis for manipulator development on new aircraft in fixed-base simulators.

Neuromuscular system induced roll ratchet appears more likely in rolls to the right (for right-hand side stick) because the pilot must develop most of the force applied to the stick with the thumb. The greater muscular tension required increases the neuromuscular peaking and hence the tendency to roll ratchet. Since the pilot cannot generate as high a force level with the thumb as with the palm of the hand, there also may be a tendency to hold a given maneuver force a few seconds longer in right rolls and therefore make the ratchet more noticeable. Presumably the opposite tendency would occur for left-hand sticks, such as proposed for the A320.

The use of sensed stick force as the input to a high performance roll rate command augmentation system appears particularly sensitive to pick-up of the neuromuscular system dynamic peaking. Prevention of such pick-up requires a relatively low frequency first-order lag filter which may result in objectionably sluggish (PIO prone) roll rate response. There appears to be a relatively narrow band of acceptable filter time constants defined by these two high and low frequency PIO type responses. The simulation results also show a rather narrow band for acceptable roll rate command/force gradient. This is most apparent for fixed (no displacement) type manipulators. Comparison between simulator and flight results tend to show these findings apply to center as well as side-stick manipulators.

With stick force sensing, the neuromuscular peaking, roll ratchet tendency, and command gradient sensitivity can be minimized by

- providing the manipulator with a moderate amount of deflection (0.7-0.8 deg/lb appears to be a desirable range).
- minimizing flight control system time delay, $\tau < 50$ msec.
- placing the effective roll response time constant in the range $0.2 < T < 0.3$ sec.
- maintaining the response/force gradient in the range $10 < K_c < 20$ deg/sec/lb.

A recapitulation of detailed conclusions relative to human pilot dynamic characteristics is given below. These specialize, and to some extent duplicate, the broader conclusions given above.

1. Crossover Model Refinements

   - The property $\omega_c(Y_c)$ = constant extends over an order of magnitude variation in K_c changes in force gradient. ω_c begins to fall off as very small K_c demand great pilot effort (large K_p) to keep ω_c constant.
   - Controller element lags for $Y_c = K_c/(Ts + 1)$ are:
     -- almost exactly cancelled by pilot lead when $T > 0.2$ second (lag breakpoint of 5 rad/sec);
     -- partly offset by pilot lead of approximately 1/8 second when $T \leq 0.2$ second.

     Thus the adjustment rule indicating that pilot lead will offset controlled element lags by nearly exact cancellation now has a lower limit at about 1/8 second.

2. Human Pilot Limb-Manipulator Dynamics

   - The classical third-order system approximation for the limb-manipulator portion of the human neuromuscular system is both adequate and an essential minimum form needed to consider pilot-aircraft system dynamic interactions in the frequency range from 8-20+ rad/sec.

REFERENCES

1. Magdaleno, Raymond E., Duane T. McRuer, and George P. Moore, Small Perturbation Dynamics of the Neuromuscular System in Tracking Tasks, NASA CR-1212, Dec. 1968.

2. Magdaleno, R. E., and D. T. McRuer, Experimental Validation and Analytical Elaboration for Models of the Pilot's Neuromuscular Subsystem in Tracking Tasks, NASA CR-1757, Apr. 1971.

3. McRuer, D. T., L. G. Hofmann, H. R. Jex, et al., New Approaches to Human-Pilot/Vehicle Dynamic Analysis, AFFDL-TR-67-150, Feb. 1968.

4. McRuer, D. T., and E. S. Krendel, Mathematical Models of Human Pilot Behavior, AGARDograph No. 188, Jan. 1974.

5. Harper, Robert P., Jr., In-Flight Simulation of the Lateral-Directional Handling Qualities of Entry Vehicles, Calspan Report No. TE-1243-F-2, Feb. 1961.

6. Monagan, Stephen J., Rogers E. Smith, and Randall E. Bailey, Lateral Flying Qualities of Highly Augmented Fighter Aircraft, AFWAL-TR-81-3171, Mar. 1982.

7. Smith, R. E., Evaluation of F-18A Approach and Landing Flying Qualities Using an In-Flight Simulator, Calspan Report No. 6241-F-1, Feb. 1979.

8. Chalk, C. R., "Excessive Roll Damping Can Cause Roll Ratchet," J. Guidance, Control, and Dynamics, Vol. 6, No. 3, May-June 1983, pp. 218-219.

9. Mitchell, D. G., and R. H. Hoh, "Flying Qualities Requirements for Roll CAS Systems," AIAA Paper 82-1356, presented at the AIAA 9th Atmospheric Flight Mechanics Conference, San Diego, CA, 9-11 Aug. 1982.

10. Allen, R. Wade, Henry R. Jex, and Raymond E. Magdaleno, Manual Control Performance and Dynamic Response During Sinusoidal Vibration, AMRL-TR-73-78, Oct. 1973.

11. Gordon-Smith, M., An Investigation into Certain Aspects of the Describing Function of a Human Operator Controlling a System of One Degree of Freedom, Univ. of Toronto, UTIAS Rept. No. 149, Feb. 1970.

12. Magdaleno, R. E., and D. T. McRuer, Effects of Manipulator Restraints on Human Operator Performance, AFFDL-TR-66-72, Dec. 1966.

- The peaking tendency (damping ratio, ζ_N) of the quadratic component of the third-order approximation is a very strong function of the controlled element dynamics -- in essence this feature can be "tuned" by adjusting controlled element properties.

- For all stick force/displacement characteristics investigated the highest ζ_N (smallest peaking tendency) occured for $Y_c = K_c/s$ controlled elements.

- There is only marginal difference between peaking tendencies associated with a controlled element $K_c/s(0.1s + 1)$ and a pure K_c/s.

- Pure time delay induces a greater peaking tendency than an equivalent time lag.

- Distinct peaking tendencies occured for fixed and small deflection sticks for $\tau = 0.07$ and 0.1 second.

- The controlled element form which exhibited the maximum peaking tendency ($\Delta AR = 7$ dB) was $Y_c = K_c e^{-\tau s}/s$, for $\tau = 0.07$ sec. Higher and lower values of τ resulted in less peaking.

- For large deflection sticks the peaking tendency is minimized or non-existent.

13. McRuer, D. T., and R. E. Magdaleno, Human Pilot Dynamics with Various Manipulators, AFFDL-TR-66-138, Dec. 1966.

14. Garland, Michael P., Michael K. Nelson, and Richard C. Patterson, F-16 Flying Qualities with External Stores, AFFTC-TR-80-29, Feb. 1981.

15. Magdaleno, Raymond E., Henry R. Jex, and R. Wade Allen, "Modeling and Measuring Limb Fine-Motor Unsteadiness," Systems Technology, Inc., P-136, presented at the Ninth Annual Conference on Manual Control, Cambridge, MA, 23-25 May 1973.

16. Hall, G. Warren, and Rogers E. Smith, Flight Investigation of Fighter Side-Stick Force-Deflection Characteristics, AFFDL-TR-75-39, May 1975.

1. Report No. NASA CR-3983	2. Government Accession No.	3. Recipient's Catalog No.
4. Title and Subtitle Investigation of Interactions Between Limb-Manipulator Dynamics and Effective Vehicle Roll Control Characteristics		5. Report Date May 1986 6. Performing Organization Code
7. Author(s) D.E. Johnston and D.T. McRuer		8. Performing Organization Report No. H-1320 10. Work Unit No. RTOP 505-67
9. Performing Organization Name and Address Systems Technology, Inc. 13766 South Hawthorne Boulevard Hawthorne, California 90250		11. Contract or Grant No. NAS2-11454 13. Type of Report and Period Covered Contractor Report-Final
12. Sponsoring Agency Name and Address National Aeronautics and Space Administration Washington, D.C. 20546		14. Sponsoring Agency Code

15. Supplementary Notes

NASA Technical Monitor: Donald T. Berry, Ames Research Center, Dryden Flight Research Facility, Edwards, California 93523-500

16. Abstract

A fixed-base simulation was performed to identify and quantify interactions between the pilot's hand/arm neuromuscular subsystem and such features of typical modern fighter aircraft roll rate command control system mechanizations as: (1) force sensing side-stick type manipulator, (2) vehicle effective roll time constant, and (3) flight control system effective time delay.

The simulation results provide insight to high frequency PIO (roll ratchet), low frequency PIO, and roll-to-right control and handling problems previously observed in experimental and production fly-by-wire control systems. The simulation configurations encompass and/or duplicate several actual flight situations, reproduce control problems observed in flight, and validate the concept that the high frequency nuisance mode known as "roll ratchet" derives primarily from the pilot's neuromuscular subsystem. The simulations show that force-sensing side-stick manipulator force/displacement/command gradients, command prefilters, and flight control system time delays need to be carefully adjusted to minimize neuromuscular mode amplitude peaking (roll ratchet tendency) without restricting roll control bandwidth (with resulting sluggish or PIO prone control).

The results further demonstrate that roll ratchet tendency, which is difficult to detect in fixed-base simulations, is readily apparent from application of frequency response spectral analysis techniques. Consequently the application of appropriate spectral measurement techniques during flight control system design/development piloted simulation phases promise to reduce later and more costly flight test investigation.

17. Key Words (Suggested by Author(s))	18. Distribution Statement
Flying qualities Limb-manipulator dynamics Neuromuscular system Roll control	Unclassified — Unlimited STAR category 08

19. Security Classif. (of this report)	20. Security Classif. (of this page)	21. No. of Pages	22. Price*
Unclassified	Unclassified	64	A04

For sale by the National Technical Information Service, Springfield, Virginia 22161.

NASA-Langley, 19